PERFORMANCE ANALYSIS OF ADAPTIVE

MODULATION AND MIMO SYSTEMS

APPLYING MACROSCOPIC DIVERSITY

TECHNOLOGIES

By

YUAN ZHANG

Bachelor of Engineering
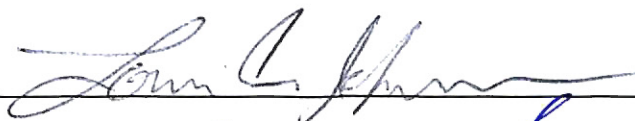
Wuhan University of Technology

HuBei, China

2001

Submitted to the Faculty of the
Graduate College of the
Oklahoma State University
in partial fulfillment of
the requirements for
the degree of
MASTER OF SCIENCE
July, 2004

PERFORMANCE ANALYSIS OF ADAPTIVE

MODULATION AND MIMO SYSTEMS

APPLYING MACROSCOPIC DIVERSITY

TECHNOLOGIES

Thesis Approved:

_____

Thesis Advisor

_____

_____

_____

Dean of the Graduate College

PREFACE

Nowadays, wireless communication engineers are being challenged by the request of high speed data services anywhere anytime but still constrained by limited power and frequency bandwidth requirements. Several promising technologies have been given much attention. In this thesis, three of those are introduced and optimized, which are multiple input multiple output (MIMO) antennas systems, macroscopic diversity schemes and adaptive modulation technologies. The objective of this thesis is to investigate methods that can increase the data rate or spectral efficiency and optimize the system performance through combined techniques.

In Chapter 2, some basic concepts related to the research are introduced, such as Rayleigh fading, log-normal shadowing, receiver diversity combining schemes, and outage probability. Then the literature review of the above mentioned three techniques follows.

Chapter 3 introduces the MIMO system in detail. It begins with the channel capacity equation of MIMO systems. Two kinds of channel models, one ring model and correlation matrix model, are represented and analyzed. The correlation matrix model is a generic one that includes several fading situations. It also includes the one ring model. Besides that, channel decomposition is introduced to represent the channel capacity of the MIMO system as the capacity summation of several single antenna systems. The water-filling power allocation strategy can increase the channel capacity further if the channel

varying information is known at the transmitter side. After that, the macroscopic MIMO system is proposed. The performance improvement obtained compared to applying the single base station MIMO system is shown.

Adaptive modulation has been studied intensively in Chapter 4. By applying the probability density function (PDF) of the signal to noise ratio (SNR) of the macroscopic selection diversity system under a composite fading environment, the spectral efficiency of adaptive macroscopic selection diversity systems under different constraints are investigated. The adaptive macroscopic maximum ratio combining system is also proposed which results in the best spectral efficiency performance.

The conclusion and references are given in Chapter 5 and Chapter 6, respectively.

ACKNOWLEDGMENTS

TABLE OF CONTENTS

LIST OF FIGURES

LIST OF SYMBOLS AND ABBREVIATIONS

Symbol / Abbreviation

AWGN	Additive white Gaussian noise
BER	Bit error rate
BPSK	Binary phase shift keying
BS	Base station(s)
C	Capacity or spectral efficiency
CDF	Cumulative distribution function
CDI	Channel distribution information
C-Rate A-BER	Continuous Rate and Average BER
C-Rate I-BER	Continuous Rate and Instantaneous BER
CSI	Channel state information
D_H	Eigenvalues of channel matrix
D-Rate A-BER	Discrete Rate and Average BER
D-Rate I-BER	Discrete Rate and Instantaneous BER
f_c	Carrier frequency
g	Channel power gain
H	Channel matrix of MIMO system
H_w	Complex i.i.d. Rayleigh random channel matrix
i.i.d.	Independent identically distributed
$k(\gamma)$	Data rate for a specific SNR
L	The number of base stations
M	The number of transmit antennas at one base station
m	Mean value

MDC	Macroscopic diversity combining
MIMO	Multiple input and multiple output
MRC	Maximum ratio combining
MU	Mobile user
N	The number of receiver antennas for one user
P	Probability
P_T	Total transmit power
$p(\gamma)$	PDF of SNR
PDF	Probability Density Function
Q	Input covariance matrix
QAM	Quadrature Amplitude Modulation
QoS	Quality of Service
R	Correlation matrix of antenna array
S	The number of scatterers
$\overline{S}$	Average transmit power
$S(\gamma)$	Transmit power for a specific SNR
$S(\theta)$	The effective scatterer located at angle θ
SISO	Single input and single output
SNR	Signal to noise ratio
SVD	Singular Value Decomposition
V	Single vector
α	Signal envelope
γ	SNR
λ	Radio wavelength
μ	Water-fill level
τ	Time delay
σ^2	Variance of random variable
ω	Log-normal fading component
Δ	Angle spread
Θ	Angle of arrival

Ω	Log-normal fading matrix for the macroscopic system
Ω_θ	The angle at which $S(\theta)$ is situated
Ψ	Covariance matrix of H

Chapter 1

Introduction

1.1 Overview

Wireless communication systems are extensively used in peoples' lives. With the request of high data rates and wireless multimedia services, engineers are being challenged by limited power and bandwidth constraints. In order to provide high-speed and robust wireless multimedia communication services on the scarce frequency spectrum, technologies that can guarantee a certain level of Quality of Service (QoS) and spectrum efficient transmission becomes extremely important.

In the recent past years, numerous investigations have been conducted on several promising techniques, such as multiple input multiple output (MIMO) antennas systems, adaptive modulation technologies, and macroscopic diversity schemes. In this thesis, these three technologies are intensively studied and improved combined system models are developed and analyzed. The objective of the research is to combine these technologies and to further increase the data rate by efficient usage of the time, frequency, and space domain. Two kinds of systems are introduced in this thesis, which are the macroscopic diversity MIMO system and adaptive macroscopic diversity system. In the second part of this thesis, the performance of the adaptive macroscopic selection diversity scheme and the adaptive macroscopic maximum ratio combining scheme are investigated.

The performance analysis is conducted in terms of spectral efficiency, whose unit is bps/Hz. The results of the study show that the spectral efficiency can be increased significantly by effectively combining these technologies together.

1.2 Basic Introduction

1.2.1 MIMO Technology

Nowadays, MIMO wireless systems, which deploy multiple antennas at the transmitter and receiver, are being studied extensively. Multiple receive antennas provide diversity gain, while multiple transmit antennas offer multiplexing gain. Thus, it becomes a highly promising technique to support new wireless applications. Pioneering work by Winter [1], Foschini [2], and Telatar [3] showed that, for single-user systems, the maximum achieved capacity can be increased almost linearly when the number of transmit antennas and receive antennas are increased. Especially, when the channels experience independent fading, i.e., the channel matrix has full rank, the MIMO channels can be decomposed into several independent single-input single-output (SISO) channels. The capacity is obtained from the summation of the capacity of those SISO channels.

1.2.2 Macroscopic Diversity Scheme

Macroscopic diversity is a technique to increase the channel information capacity in a rich scattering fading environment. The rich scattering environment means that the communication channels experience fast fading (i.e., Rayleigh fading) and slow fading (i.e., log-normal shadowing). This phenomenon is referred to as composite fading. In other words, slower changing terms which are due to the shadowing effects from obstacles are superimposed on the rapid fluctuations that are from multipath effects. By

deploying several base stations to support a single cell, we can combat the variations of the mean signal level introduced by the log-normal shadowing effect. This is due to the fact that we can utilize the wireless channel links which are in the best condition to decode the signal. The signals from different base stations that are located at quite a distance from each other are independent, therefore the macroscopic diversity scheme can mitigate the slow fading component. As a result, the bit error rate (BER) and the stability of the link connection of the system can be improved.

1.2.3 Adaptive Modulation

Adaptive modulation is a promising technique to maximize the data rate and provide reliable QoS support over fading channels. It allocates all possible resources dynamically based on the channel information fed back to the transmitter. The basic idea is to assign more data on the channel that is in a good condition and less data on the channel that experiences a degraded quality, and in some cases the transmitter will not send at all when an extremely distorted channel is experienced. This decision is based on the transmit power, constellation size, BER, or any combination of these criteria [4], [5]. This means that the adaptive modulated systems can allocate the resources dynamically based on the channel state information (CSI) such that the channels can be utilized optimally.

1.3 Significance of the Research

This thesis focuses on three promising techniques which can improve the spectral efficiency of wireless communication systems. As mentioned in the next chapter, the

combination of those technologies to further optimize the spectral efficiency further has not been conducted yet in the existing literature. After an intensive background study, two kinds of systems are proposed. One is the macroscopic diversity MIMO system, which deploys several base stations to support one cell and has several antennas at each base station. In this system, multiple antennas of one base station can mitigate the fast fading, while several base stations can be used to combat the slow fading (details are given in Chapter 3). As shown in Chapter 3, such a system can significantly increase capacity compared to the non-macroscopic MIMO system configuration. It is worthwhile to notice that applying the macroscopic diversity technique in MIMO systems does not increase the complexity of hardware implementation, because it just changes the way that the systems process the additional channels. In other words, the macroscopic scheme can provide an increase in the capacity without increasing the complexity of implementation. Another system introduced is the adaptive macroscopic diversity system. In this category, two subsystems are investigated. One is the adaptive macroscopic selection diversity system, the other one is the adaptive macroscopic maximum ratio combining system. By combining the adaptive modulation and macroscopic diversity scheme together, significant improvements in spectral efficiency can be obtained compared to the adaptive modulation on a single base station system. These results have a great significance when it comes to the design of future broadband wireless mobile communication systems.

1.4 Methodologies Used in This Research

Monte Carlo simulation is a common applied method in complex system performance analysis. In MIMO systems, it can be used to generate one realization of a

channel matrix, and then repeat this procedure numerous times to provide the accurate channel statistics. By assuming the fading channel is an ergodic stochastic process, calculating the capacity based on each realization and averaging the results can produce the ergodic mean channel capacity. This approach can also be used in evaluating the performance of the macroscopic diversity combining system.

Another mathematical tool that has been investigated is the two-dimensional bisection method studied in [5]. In order to find the proper Lagrange parameters (λ_1 and λ_2), a two-dimensional bisection method is used to do the balance job. The details are given in Chapter 4.

Chapter 2

Basic Concepts and Literature Review

In this Chapter, some basic concepts related to the research are introduced in the first section. These are the channel fading models, receiver diversity schemes and outage definitions. After that, the literature reviews for MIMO technology, macroscopic diversity, and adaptive modulation are presented.

2.1 Basic Concepts of the Research

2.1.1 Fading Models

A. Rayleigh Rading

In a typical wireless communication environment, the transmitted signal experiences scattering, reflecting, and diffraction. Therefore, at the receiver side, the same reflected signal will arrive from multiple different paths with different delays. The corresponding time-variant channel impulse response can be expressed as [6]

$$c(\tau,t) = \sum_n \alpha_i(t) e^{-j2\pi f_c \tau_i(t)} \delta[\tau - \tau_i(t)] \qquad (2.1)$$

where n is the number of multipath, α_i is the attenuated amplitude of the ith path, and $\tau_i(t)$ is the time delay compared to the first arriving signal component of the ith path, and f_c is the carrier frequency.

When there are a large number of paths existing in the channel, $c(\tau,t)$ can be modeled as a zero-mean complex-valued Gaussian process [6]. That means the envelope will be $|c(\tau,t)| = \sqrt{c_x + c_y}$, where c_x and c_y are zero-mean Gaussian random variables. Then the envelope $|c(\tau,t)|$ is Rayleigh distributed. Such a fading channel is called a Rayleigh fading channel. The probability density function (PDF) of a Rayleigh distribution is

$$p_c(r) = \frac{r}{\sigma^2} e^{-r^2/2\sigma^2} \tag{2.2}$$

where σ^2 is the variance of the envelope. Usually the variances of c_x and c_y are set to 0.5, such that σ^2 is normalized to 1.

B. Log-normal Shadowing

In wireless communication systems, especially in the outdoor wireless environment, the communication links are blocked or scattered by some big obstacles, such as mountains, skyscrapers, etc. This makes the mean signal level fluctuate slowly when compared to the Rayleigh fading (i.e., fast fading). This is called shadowing effect or slow fading. It can be expressed as a log-normal distributed variable.

Let L be a log-normal random variable and

$$X = 10\log_{10} L \tag{2.3}$$

where X is normally distributed with PDF

$$p_X(x) = \frac{1}{\sqrt{2\pi}\sigma_x} \exp\left[\frac{-(x-m_x)^2}{2\sigma_x^2}\right] \tag{2.4}$$

where m_x and σ_x are the mean and the standard deviation of X, respectively. Thus, the PDF of L can be obtained as [7]

$$p_L(u) = \frac{1}{\sqrt{2\pi}\sigma_L} \exp\left[\frac{-\ln^2(u/m_L)}{2\sigma_L^2}\right] \qquad (2.5)$$

where $\ln(m_L) = \lambda m_x$, $\sigma_L = \lambda\sigma_x$ and $\lambda = \ln(10)/10 \approx 0.23$.

C. Composite Fading

A real wireless communication channel consists of the above two kinds of fading. This is particularly true for the case of slow moving or stationary mobile users [8]. The instantaneous channel amplitude varies very quickly as a Rayleigh-distributed random variable, while the mean value of the amplitude fluctuates slowly and follows a log-normal distribution. The received composite signal can be expressed as the product of the Rayleigh fading component and the log-normal shadowing component [9].

$$\alpha(t) = \alpha_R(t) \cdot \alpha_L(t) \qquad (2.6)$$

where $\alpha_R(t)$ is the Rayleigh fading component and $\alpha_L(t)$ is the log-normal shadowing component.

2.1.2 Diversity Schemes

In order to compensate for the channel fading, diversity schemes have been proved to be a very effective method. It provides the receiver with multiple replicas of the same information signal such that the error probability is minimized dramatically and the data rate can be increased. There are different diversity methods, and those techniques can fall

8

into seven categories: 1) space diversity, 2) angle diversity, 3) polarization diversity, 4) field diversity, 5) frequency diversity, 6) multipath diversity, 7) time diversity [8].

In this thesis, only space diversity is investigated. It is achieved by using multiple transmit antennas or receive antennas, like the MIMO system. This section discusses a diversity combining scheme for a system with a single transmit antenna and multiple receive antennas. Diversity combining can take place at the passband, called predetection combining; combining that takes place at the baseband is called postdetection combining. The postdetection combining implementation is considered in this thesis. The illustration of the receiver diversity combining is shown in Fig. 2.1.
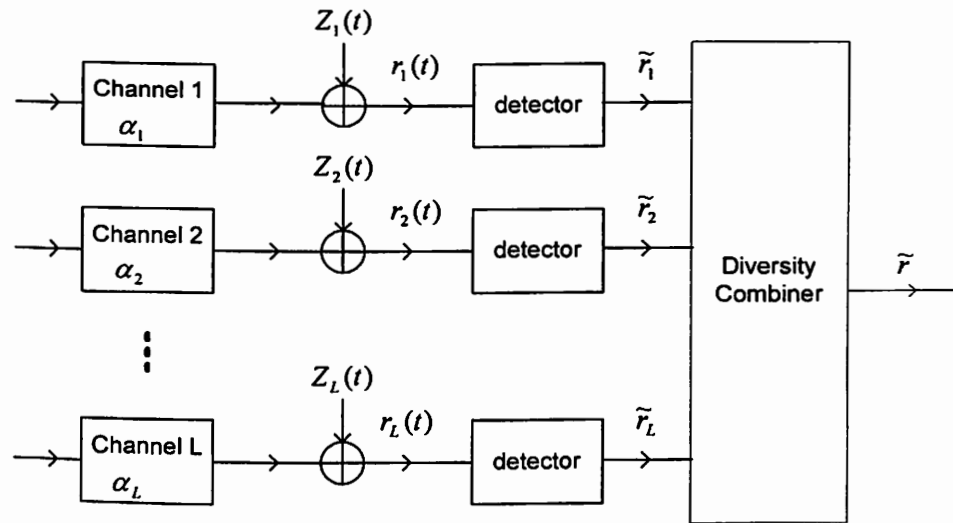
Fig. 2.1 Receiver combining architecture.

In Fig. 2.1, there are L diversity branches, α_L is the channel fading of the L th path. Here the phase delays of the channel are assumed to have been cancelled by each other. $Z_k(t)$ is the additive white Gaussian noise (AWGN) and $r_k(t)$ is the complex envelope of the received signal, where $k = 1, \cdots, L$. The term $\tilde{r}_k$ is the corresponding received signal

vector, and $\tilde{r}$ is the final signal vector corresponding to different diversity schemes. $r_k(t)$ can be expressed as

$$r_k(t) = \alpha_k S(t) + Z_k(t) \qquad k = 1, \cdots, L \qquad (2.7)$$

where $S(t)$ is the transmitted signal at the time index t. As we know, the branch correlation will reduce the achievable diversity gain. To simplify the analysis, the diversity branches are assumed to be uncorrelated.

Now, three existing receiver diversity combining schemes are introduced, which are selection diversity, maximum ratio combining (MRC), and equal gain combining.

A. Selection Diversity

The selection diversity scheme chooses the wireless link yielding the highest signal-to-noise ratio (SNR). In this case, the diversity combiner performs the following operation

$$\tilde{r} = \max_{|\alpha_k|} \tilde{r}_k \qquad k = 1, \cdots, L \qquad (2.8)$$

The SNR of the ideal selection diversity system is given as

$$\gamma_{SC} = \frac{[\alpha_{k,\max} S(t)]^2}{[Z(t)]^2} = (\alpha_{k.\max})^2 \cdot \frac{E_g}{\sigma_N^2} = \gamma_{k,\max} \qquad (2.9)$$

where E_g is the received signal power for the ideal channel and σ_N^2 is the variance of the AWGN. Therefore, $\dfrac{E_g}{\sigma_N^2}$ is the average SNR. The selection diversity is the simplest macroscopic receiver scheme.

B. Maximum Ratio Combining

In the maximum ratio combining scheme, all wireless links are weighted by their respective complex channel gains and then are combined. Referring to Fig. 2.1, the output of the combiner is expressed as

$$\tilde{r} = \sum_{k=1}^{L} \alpha_k^* \tilde{r}_k \tag{2.10}$$

where α_k^* is the conjugate of the respective complex channel fading gain. Then the SNR of the MRC scheme is

$$\gamma_{MRC} = \frac{\left[S(t) \sum_{k=1}^{L} \alpha_k^2 \right]^2}{[Z(t)]^2 \sum_{k=1}^{L} \alpha_k^2} = \frac{E_g}{\sigma_N^2} \sum_{k=1}^{L} \alpha_k^2 = \sum_{k=1}^{L} \gamma_k \tag{2.11}$$

As an observation, the SNR of the MRC scheme is equal to the summation of the SNR of each branch.

C. Equal Gain Combining

The equal gain combining scheme is easier to implement compared to the MRC scheme, but does not provide an optimal performance. This scheme does not weight the wireless link channel gain, but just combines all the link signals together and conducts the detection. The SNR of equal gain combining scheme results in

$$\gamma_{EGC} = \frac{\left[S(t) \sum_{k=1}^{L} \alpha_k \right]^2}{\sum_{k=1}^{L} [Z(t)]^2} = \frac{E_g (\sum_{k=1}^{L} \alpha_k)^2}{L \cdot \sigma_N^2} \tag{2.12}$$

D. Performance Comparison of Diversity Combining Schemes

In order to compare the performance of the above three different diversity combining schemes, the BER probabilities of different diversity combining schemes for Binary Phase Shift Keying (BPSK) system with AWGN channels are shown in Fig. 2.2. It is observed that adding one additional branch gives a significant improvement of system performance compared to the single receive antenna system, no matter which diversity scheme is chosen. Comparing the three diversity schemes, MRC gives the best performance. This is because each branch is weighted by its channel gain which would proportionally strengthen the good signals, while weakening the poor signals. Since the selection diversity scheme just selects one branch which has the highest SNR and discards the rest of them, it has the worst system performance. The performance of the equal gain combining is between the MRC and selection diversity schemes.
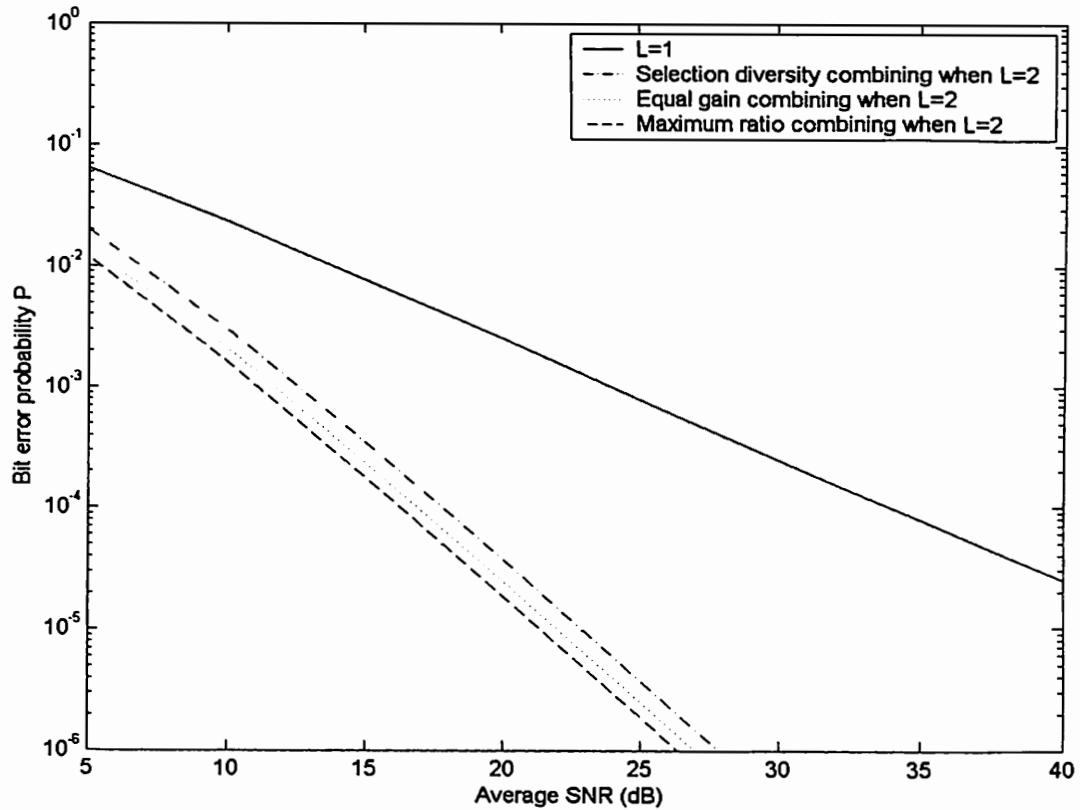
Fig. 2.2 BER probabilities of different diversity schemes for the BPSK system with

AWGN channels.

2.1.3 Outage Definitions

A. Definition of Outage

The outage defined in telecommunication systems is the probability that the system

service condition in which a user is completely deprived of service by the system or the

probability that the system condition is below a defined system threshold [10].

This threshold could be noise power, data rate or even BER constraint. Here, the

outage applications are categorized into two main groups. One is based on the constraint

of the signal-to-noise ratio, signal-to-interference-noise ratio, or noise power; the other one is based on the data rate threshold.

B. Outage Based on SNR

As mentioned in [8], the outage is defined as the probability that the carrier-to-noise ratio or carrier-to-interference ratio or both is less than the thresholds. In [11] and [12], the outage is the probability that the ratio of desired signal power to all interference power is less than a constant value, which is a protection parameter required for reliable communication. It can be expressed as:

$$P\left(\frac{P_{s0}}{P_{sn}} < \alpha\right) \qquad (2.13)$$

where $P(\cdot)$ means probability, P_{s0} is the signal power, P_{sn} is the all interference power and α is the protection threshold.

C. Outage Based on the Given Data Rate

The most common definition of outage is based on the data rate. The outage capacity can be achieved with the error probability

$$P = P(C_i < C_p) \qquad (2.14)$$

where C_i is the instantaneous data rate and C_p is the outage capacity or spectral efficiency with P outage probability [13]. The papers [14]-[18] use a similar definition. In [19], the outage probability should also satisfy the power constraint as well as the data rate. It is given as:

$$P(R, p) = \inf_{\{Q \geq 0, trace(Q) \leq p\}} P(\log \det(I_n + HQH^+) < R) \qquad (2.15)$$

14

where Q is the correlation matrix of the input information, p is the power constraint, H is the channel matrix, and I_n is the identity matrix with the dimension n. R is the given data rate as threshold.

The BER constraint can also be included in the outage probability definition, which means that under a total power constraint and given BER constraint, outage is the probability that the data rate is less than C_p.

2.2 Literature Review for This Research

2.2.1 Literature Review on MIMO Technology

As mentioned in the introduction, MIMO systems have a much higher data rate because multiple antennas provide multiplexing gain besides the diversity gain. Therefore, the MIMO capacity can be the summation of capacities of each single channel if those channels are uncorrelated to each other. Unfortunately, it is not a practical model in a real communication environment. Much work has been done to analyze the performance of MIMO channels under more realistic conditions, like the fading and the channel correlated environment.

From [20], we know that the MIMO channel capacity highly depends on the statistical properties and antenna element correlations of the channel. When the instantaneous channel gains, called the channel state information (CSI), are known at both the transmitter and the receiver, the transmitter can adjust its transmission strategy adaptively based on the instantaneous CSI. When only the channel distribution is known at the transmitter, called the channel distribution information (CDI), the transmitter must maintain a fixed-rate transmission with respect to the CDI. This fixed-rate depends on the

eigenvectors and eigenvalues of the channel covariance matrix. In [21], the authors showed the advantages of ideal MIMO channels by assuming independent Rayleigh fading channels with known shadowing components. [22] provides a comprehensive introduction of MIMO communication systems, such as the one ring model, power allocation strategy, and space-time code architecture. The MIMO study of this research refers to this reference. An important covariance matrix representation of the MIMO channel is given in [23]. The correlation is characterized by the angle spread, antenna space, and scattering environment. This general model is applicable to models that vary from an independent identically distributed (i.i.d.) Gaussian model to the totally correlated case depending on the scattering radius, antenna beamwidths and spacing, which has been validated by measurements in actual cellular systems in [24]. The space-time coding scheme is another promising technology to approach the theoretical capacity limits. It transmits redundant information on parallel antennas to obtain the diversity gain [25]. More details and corresponding assumptions will be introduced later.

2.2.2 Literature Review on Macroscopic Diversity Technique

The original ideas of the macroscopic diversity technique are organized in [26] by Jakes. As introduced earlier, three different receiver diversity combining schemes can be used to combine the macroscopic branches. As developed in [27], all received signals are detected, and a maximum-likelihood decision algorithm is employed to maximize the probability of correct decision. The performance improvement is also shown compared to that of a macroscopic selection diversity scheme. In [28], a composite microscopic plus macroscopic diversity system is introduced. For the uplink, i.e., from the mobile user to

16

the base station, at each base station multiple antennas are deployed to deal with the fast fading components; and then the macroscopic selection diversity scheme will be performed to select the strongest signal from several base stations. After that, the BER performance of the proposed system is shown. The deviation of the PDF of an M-branch macroscopic selection diversity system under Rayleigh fading plus log-normal shadowing is demonstrated in [29]. Since there is no closed-form for that, the author used a log-normally distributed function to approximate the composite fading distribution. This is a very important result and has been used in this thesis as shown later.

2.2.3 Literature Review on Adaptive Modulation Technology

At the present time, the request for the advanced wireless systems is to provide higher QoS heterogeneous applications. High QoS means higher levels of link stability, higher data rate, lower error rate, lower jitter probability, lower outage probability, improved better handover, etc. As a result, adaptive modulation can be one solution to reach those criteria by allocating resources, such as transmit power, constellation size, and so on. In [4], the authors propose a variable-rate variable-power M-Quadrature Amplitude Modulation (QAM) system using the adaptive transmission technique. They claim that the gap between the capacity of their system and the Shannon capacity is a function of the required BER. In addition, unrestricted constellation sets achieve 1-2 dB of the spectral efficiency larger than the practical limited constellation sets. Considering transmission power, constellation size, and BER in transmission, [5] investigates adaptive modulation based on four cases in Rayleigh fading environment only: continuous rate with an average BER constraint (C-Rate A-BER), continuous rate with an instantaneous

BER constraint (C-Rate I-BER), discrete rate with an average BER constraint (D-Rate A-BER) and discrete rate with an instantaneous BER constraint (D-Rate I-BER). They also consider the constant power or constant rate case. As a conclusion, using one or two degrees of freedom in adaptive modulation yields close to the maximum spectral efficiency obtained by utilizing all the degrees of freedom. Therefore, the parameters used in adaptive transmission can be chosen based on the system implementation considerations. [30] analyzes the adaptive transmission with diversity combining techniques under Rayleigh fading channels, which is similar to this thesis' work. This thesis extends what they did to composite fading and provides other considerations.

To the best knowledge of the author, there is no paper that applies macroscopic diversity scheme into MIMO systems or combines it with adaptive modulation technology. This becomes the contribution of this thesis. It is believed that since macroscopic diversity scheme can provide additional independent channel resources, combining it with some advanced communication system or scheme will increase the spectral efficiency further.

Chapter 3

MIMO Models and the Macroscopic MIMO System

This Chapter introduces the details of the MIMO system, such as system models, the channel capacity equation, decomposition of MIMO channels and so on in section 3.1. It begins with the channel capacity equation of MIMO systems under independent fading environment. Then two kinds of channel models for MIMO systems, the one ring model and the correlation matrix model, are presented and analyzed. Besides that, channel decomposition is introduced to represent the channel capacity of a MIMO system as the capacity summation of several single antenna systems. The water-filling power allocation strategy is also shown to increase the channel capacity further if the channel varying information is known at the transmitter. In section 3.2, the macroscopic MIMO system is proposed for a given model. The performance improvement compared to the single base station MIMO system is discussed.

3.1 MIMO Models

This section presents some mathematical representations of MIMO frequency-nonselective Rayleigh fading or composite fading channels. Two useful models, one ring model and correlation matrix model, are given in detail. These two models will be used in the proposed macroscopic MIMO system.

3.1.1 Channel Model

The system considered here is a transmitter with M transmit antennas and a receiver with N receive antennas. Then the channel can be represented by a $N \times M$ matrix H. The $N \times 1$ received signal vector V equals

$$V = H \cdot S + W \tag{3.1}$$

where S is the $M \times 1$ transmitted signal vector and W is the $N \times 1$ additive white complex Gaussian noise vector, whose covariance matrix is normalized to the identity matrix.

The capacity equation for point-to-point MIMO channel is

$$C = \log_2 \left| I_N + \frac{1}{\sigma^2} HQH^+ \right| \tag{3.2}$$

where Q is the input covariance matrix $E[SS^*] = Q$, $*$ is complex conjugate operation and σ^2 is the variance of the additive Gaussian noise with the normalized variance of 1. The superscript $^+$ represents complex conjugate transpose. The trace of matrix Q equals the total transmit power P_T. The capacity in (3.2) is the capacity for one frequency unit, thus it is also called spectral efficiency. In this paper, we use these two terminologies interchangeably, whose unit is bit/s/Hz. If it is assumed that the instantaneous channel gains are independent, i.e., the elements in channel matrix H are i.i.d. complex Gaussian random variable $N(0,1)$. If the transmitter does not know the instantaneous channel gain, it will distribute the total power to all the transmit antennas equally. The equation (3.2) can be changed to

$$C = \log_2 \left| I_N + \frac{P_T}{M \cdot \sigma^2} HH^+ \right| \tag{3.3}$$

where P_T is the total transmit power.

3.1.2 Spectral Efficiency Comparison Between MIMO Systems and the Other Two Systems

The mean capacities per unit bandwidth of the MIMO system, transmitter diversity and receiver diversity under the ideal composite fading environment are compared to observe the advantages of the MIMO system. The ideal composite fading environment means transmitted signals experience Rayleigh fading plus log-normal fading, but the signals from different antennas are independent. The standard deviation of the log-normal shadowing is 8 dB and the variance of the complex Rayleigh fading is 1.

The single-user spectral efficiency of transmitter diversity can be expressed as [21]

$$C = \log_2(1 + \frac{P_T}{M\sigma^2}\sum_{m=1}^{M}|h_m|^2) \tag{3.4}$$

where M is the number of transmit antennas, and h_m is the m th fading channel gain. For the receiver diversity case, assuming the antenna array is directive, the single-user spectral efficiency is

$$C = \log_2(1 + \frac{MP_T}{\sigma^2}|h|^2) \tag{3.5}$$

where M is the number of receiver antennas.

Using Monte Carlo simulation, the mean spectral efficiencies of the transmitter diversity system, receiver diversity system, and that of the MIMO system under composite fading environment are shown in Fig. 3.1, Fig. 3.2, and Fig. 3.3, separately.
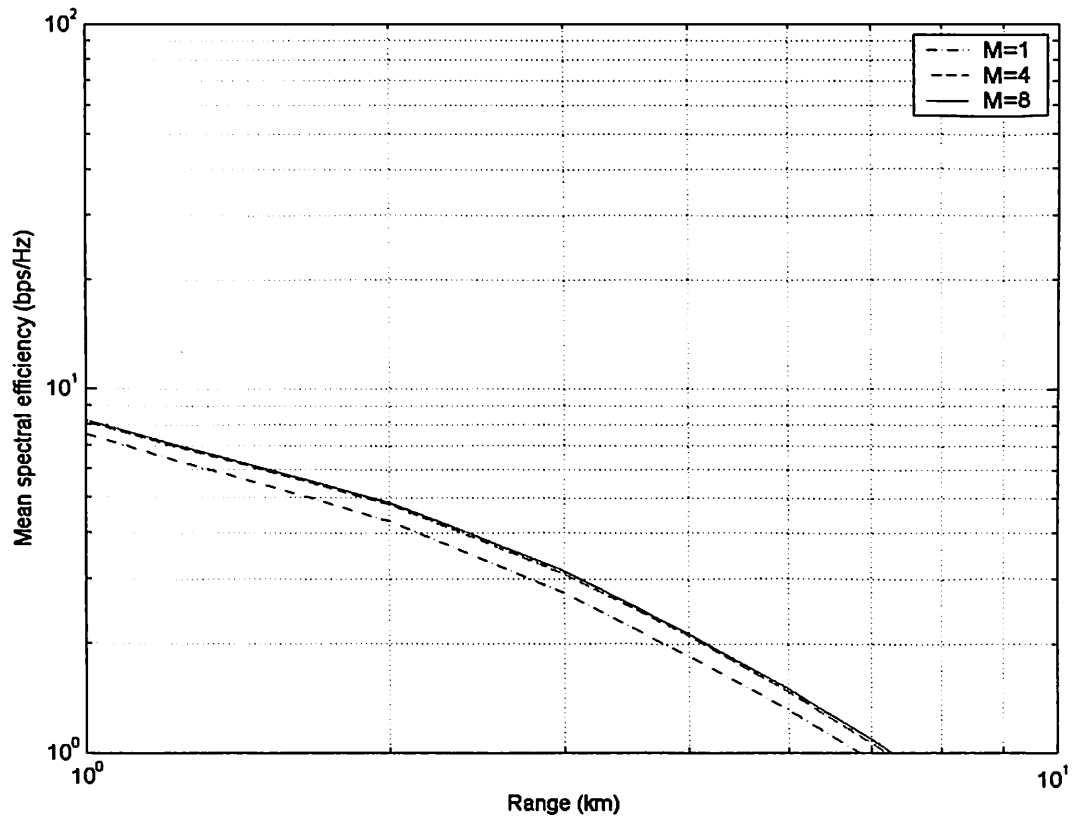
Fig. 3.1 Mean spectral efficiency of transmitter diversity system under composite fading environment versus the range between the transmitter and receiver.
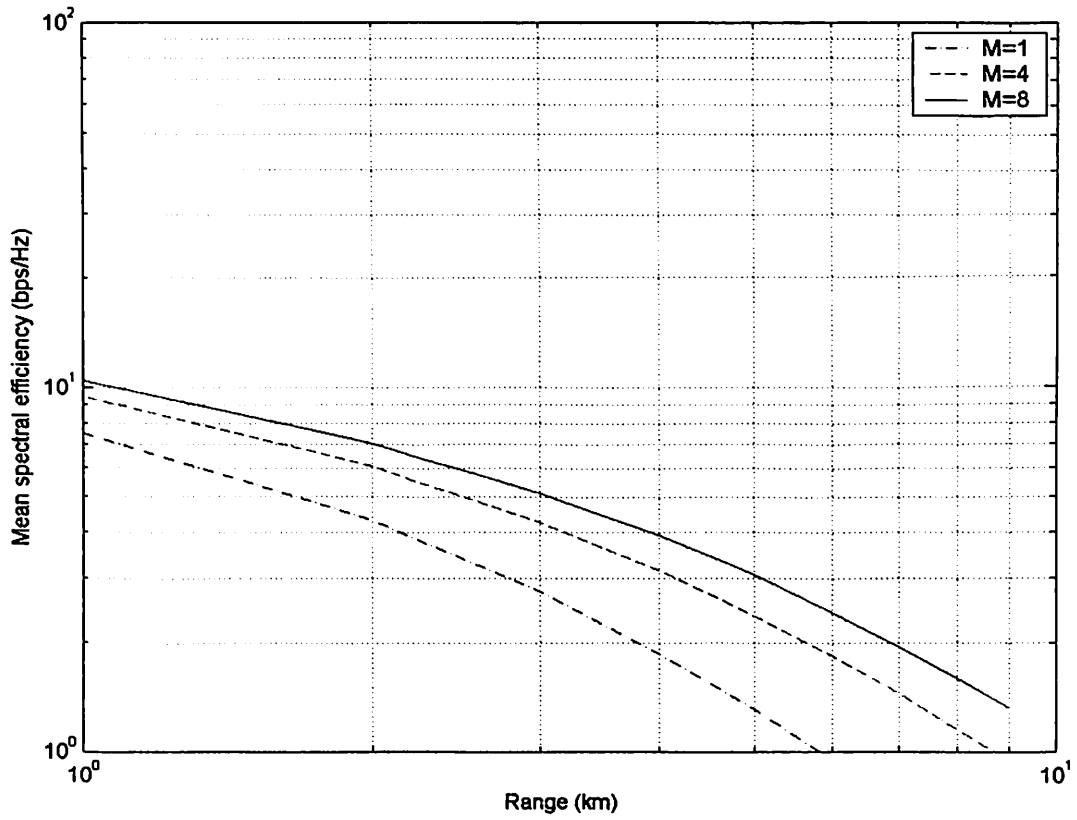
Fig. 3.2 Mean spectral efficiency of receiver diversity system under composite fading environment versus the range between the transmitter and receiver.
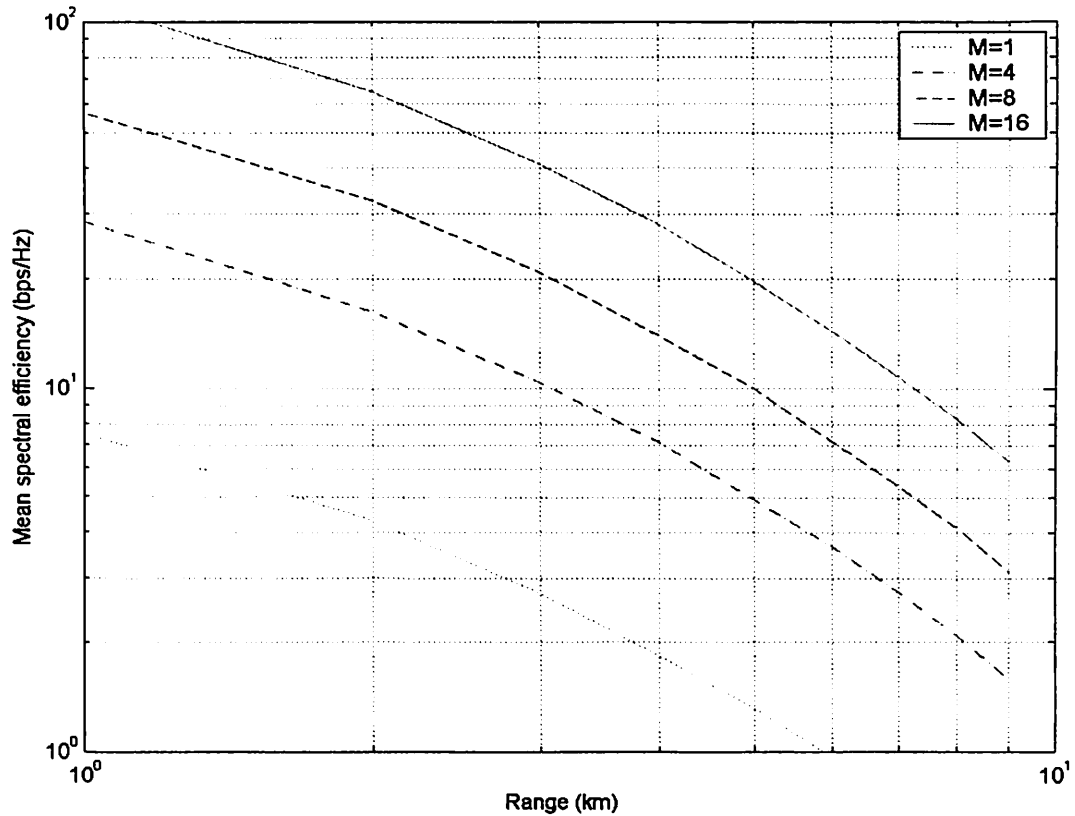
Fig. 3.3 Mean spectral efficiency of MIMO system under composite fading environment versus the range between the transmitter and receiver.

In the simulations, the total transmit power is 10 watts. M is the number of transmit antennas, receive antennas or transmit and receive antennas for each scenario respectively. From the figures, we can see that the capacity of transmitter diversity system will saturate when the number of transmit antennas is very large; the capacity of receiver diversity system increases logarithmically, while the capacity of MIMO system increases linearly.

3.1.3 One Ring Model

The discussion in the previous section is an ideal case, which gives an insight of advantages of MIMO channels. However, in a wireless propagation environment, the fading channels from different pairs are not independent, but correlated to each other. Since the mobile users (MUs) are not high enough compared to the height of base station (BS), usually a lot of buildings, cars, or even people scatter RF waves. A good model to appropriate this scattering environment is the one ring model first employed by Jakes [26]. As mentioned in [22], this model is usually used in the fixed wireless communication context, where the BS is elevated at a height such that it is unobstructed but the MU is surrounded by a local scatter ring. Based on this one ring model, the spatial fading correlation of narrowband flat fading channels can be determined from the physical parameters of the model, which include antenna spacing, antenna arrangement, angle spread, and angle of arrival. The illustration of this model is shown in Fig. 3.4 [22], where TA_p is the p th transmitting antenna, RA_l is the l th receiving antenna. $S(\theta)$ is the scatterer at angle θ. The distance between the BS and MU is D, the radius of local scatter ring is R. The angle of the incoming wave is defined within $[\Theta - \Delta, \Theta + \Delta]$, where Θ is the angle of arrival and Δ is the angle spread.
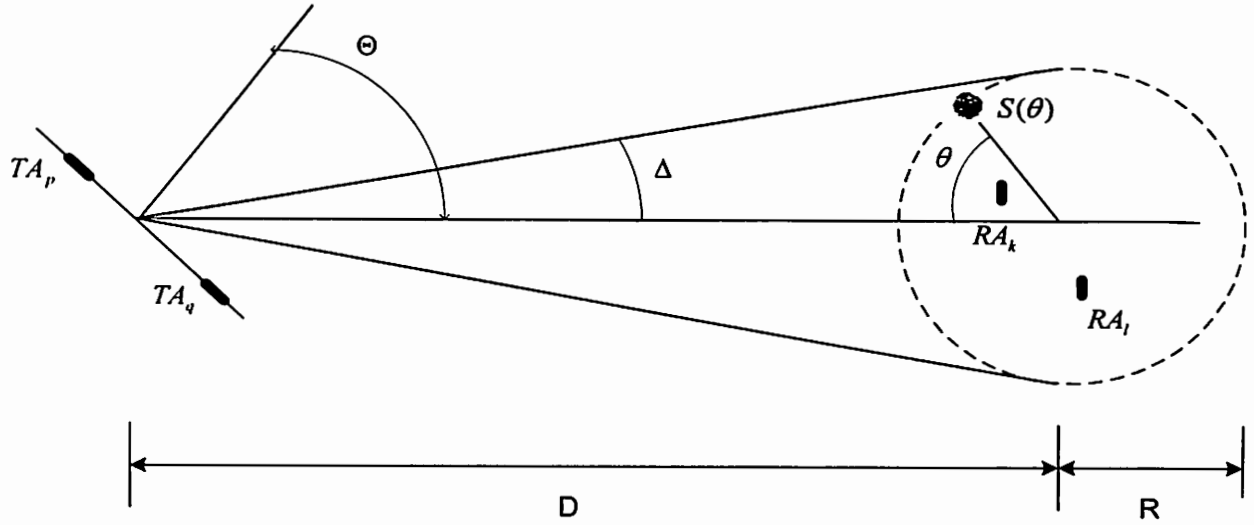
Fig. 3.4 Illustration of one ring model.

We need the following assumptions for this model:

- Actual scatterers or effective scatterers are assumed to be distributed uniformly in θ. The effective scatterer located at θ is denoted by $S(\theta)$. A phase $\phi(\theta)$ is associated with $S(\theta)$; $\phi(\theta)$ represents the dielectric properties and radical displacement from the scatterer ring of the actual scatterer that $S(\theta)$ represents. Then $\phi(\theta)$ is modeled as uniformly distributed in $[-\pi, \pi)$ and i.i.d. in θ.

- Only rays that are reflected by the effective scatterers exactly once are considered.

- All rays that reach the receiving antennas are equal in power.

- D is the distance between transmit antenna array and receiver array and R is the radius of the receiver scatterers.

After assumptions, we can get the normalized complex path gain H_p^l [22]

$$H_p^l = \frac{1}{\sqrt{2\pi}} \int_0^{2\pi} \exp\{-j\frac{2\pi}{\lambda}(D_{TAp \to S(\theta)} + D_{S(\theta) \to RAl}) + j\phi(\theta)\}d\theta \qquad (3.6)$$

26

where $D_{X \to Y}$ is the distance from object X to object Y and λ is the wavelength.

By the central limit theorem, H_p^l constructed from (3.6) is $N(0,1)$, its covariance is equal to correlation.

To study the spatial fading correlation, we use the following notation. $Vec(H)$ is used to denote the $MN \times 1$ vector. Thus if $H = (h_1, h_2, \ldots, h_M)$, where h_i is a $N \times 1$ vector for i=1,\ldots,M, then

$$Vec(H) = (h_1^{'}, h_2^{'}, \ldots, h_M^{'})^{'} \tag{3.7}$$

The covariance matrix of H is defined as the covariance matrix of the vector $Vec(H)$:

$Cov(Vec(H)) = E[Vec(H) \cdot Vec(H)^*]$. Therefore, the covariance between H_p^l and H_q^k is

$$E[H_p^l H_q^{k*}] = \frac{1}{2\pi} \int_0^{2\pi} \exp\left\{\frac{-2\pi j}{\lambda}[D_{TAp \to S(\theta)} - D_{TAq \to S(\theta)} + D_{S(\theta) \to RAl} - D_{S(\theta) \to RAk}]\right\} d\theta \tag{3.8}$$

The parameters used to derive the approximations for (3.8) are illustrated in Fig. 3.5.
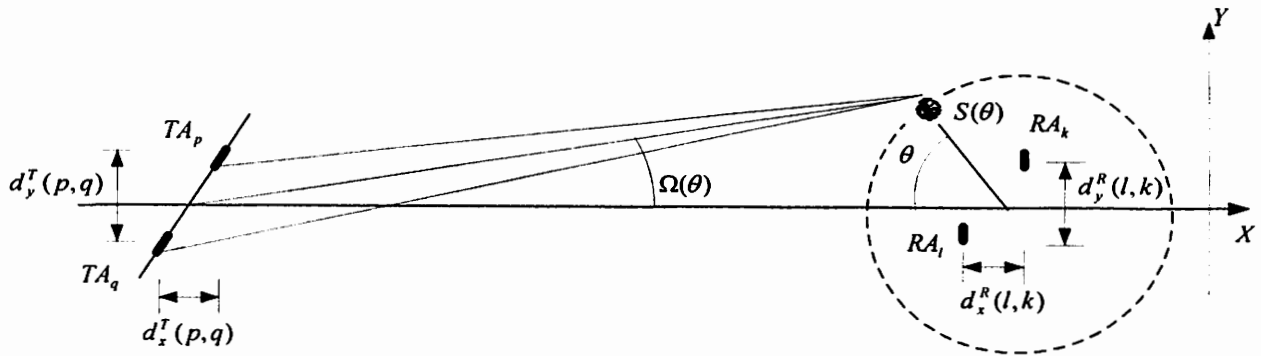
Fig. 3.5 Illustration of parameters for derivation of $E[H_p^l H_q^{k*}]$ in the one ring model.

From Fig. 3.5, when Δ is small, which is often the case in fixed wireless communication applications, we can obtain

27

$$D_{TAp \to S(\theta)} - D_{TAq \to S(\theta)} \approx d_x^T(p,q)\cos\Omega_\theta + d_y^T(p,q)\sin\Omega_\theta, \tag{3.9}$$

$$\sin\Omega_\theta \approx (R/D)\sin\theta \approx \Delta\sin\theta, \tag{3.10}$$

$$\cos\Omega_\theta \approx 1 - \frac{1}{2}(\frac{R}{D})^2\sin^2\theta = 1 - \frac{1}{4}(\frac{R}{D})^2 + \frac{1}{4}(\frac{R}{D})^2\cos 2\theta. \tag{3.11}$$

where Ω_θ is denoted as the angle at which $S(\theta)$ is situated.

Substituting these approximations into (3.8), it becomes [22]

$$E[H_p^l H_q^{k^*}] = \frac{1}{2\pi}\int_0^{2\pi}\exp\left\{\frac{-2\pi j}{\lambda}[D_{TAp \to S(\theta)} - D_{TAq \to S(\theta)} + D_{S(\theta) \to RAl} - D_{S(\theta) \to RAk}]\right\}d\theta$$

$$\approx \frac{1}{2\pi}\int_0^{2\pi}\exp\left\{-j\frac{2\pi}{\lambda}[d_x^T(p,q)(1 - \frac{\Delta^2}{4} + \frac{\Delta^2\cos 2\theta}{4}) + \Delta \cdot d_y^T(p,q)\sin\theta\right.$$
$$\left. + d_x^R(l,k)\sin\theta + d_y^R(l,k)\cos\theta]\right\}d\theta \tag{3.12}$$

If the minimum MU antenna spacing is sufficiently greater than half wavelength, the correlation introduced by a finite MU antenna element spacing is low enough such that the fades associated with two different MU elements can be considered independent. Mathematically, the N rows of H can be regarded as i.i.d. complex Gaussian row vectors with covariance matrix Ψ, where $\Psi_{p,q} = E[H_p^k H_q^{k^*}]$. The channel covariance matrix of the downlink is $Cov(Vec(H)) = \Psi \otimes I_m$, where $\otimes$ is the Kronecker product and defined as [31]

$$A \otimes B = \begin{bmatrix} A(1,1)B & A(1,2)B & ... \\ A(2,1)B & A(2,2)B & ... \\ ... & ... & ... \end{bmatrix} \tag{3.13}$$

Similarly, in the uplink $Cov(Vec(H)) = I_m \otimes \Psi$.

3.1.4 MIMO Channels Decomposition

A. Mathematical Expression

The singular value decomposition (SVD) can be used to convert the MIMO channel into $\min(M,N)$ parallel, independent SISO channels. To prove this, we first decompose channel matrix H, like $H = U_H D_H V_H^*$, and $Q = U_S D_S U_S^*$, where U_H and V_H are unitary matrixes, additionally D_H and D_S are diagonal matrixes, whose elements are singular values of the corresponding matrix. The unitary matrix has property $U^*U = I$. The equation (3.4) becomes

$$
\begin{aligned}
C &= \log_2 \left| I_N + U_H D_H V_H^* U_S D_S U_S^* (U_H D_H V_H^*)^* \right| \\
&= \log_2 \left| I_N + U_H D_H V_H^* U_S D_S U_S^* V_H D_H U_H^* \right|
\end{aligned}
\tag{3.14}
$$

We can choose $U_S = V_H$ to maximize (3.14), the capacity is changed to

$$
C = \log_2 \left| I_N + |D_H|^2 D_S \right| = \sum_{i=1}^{n=\min(M,N)} \log_2 (1 + D_S(i)|D_H(i)|^2)
\tag{3.15}
$$

where $D_S(i)$ is the transmit power for the ith SISO channel, $|D_H(i)|^2$ is the ith ordered eigenvalue of channel matrix HH^+. If the total transmit power is distributed equally to these subchannels, equation (3.15) becomes

$$
C = \sum_{i=1}^{n=\min(M,N)} \log_2 \left(1 + \frac{P_T}{n}|D_H(i)|^2 \right)
\tag{3.16}
$$

which corresponds to the equal power allocation strategy.

B. Properties of Channel Matrix's Eigenvalues

As shown in (3.16), if the equal power strategy is applied at the transmitter, the capacity of MIMO system is limited by the number of antennas and the eigenvalues of

the channel matrix. The eigenvalues of the channel matrix reflect the channel variation, correlation and attenuation, therefore further properties of those eigenvalues need to be investigated. Since $|D_H(i)|$ is the singular value of channel matrix H, $|D_H(i)|^2$ is the eigenvalue of HH^+. The magnitude of $|D_H(i)|^2$ is better displayed in decibel (dB) units [22], thus it is given as

$$\mu_k = 10\log_{10}(|D_H(k)|^2) \tag{3.17}$$

The PDF of μ_k, noted as $p_k(\mu_k)$, is used to show the properties. Monte Carlo simulation is used to generate the channel statistics, and then the ordered eigenvalues are calculated and plotted. The hexagon antenna arrays are deployed at transmitter and receiver, and the number of antennas is 7 for both sides. Since the angle spread affects the channel matrix, the PDF of the ordered eigenvalues for three different angle spread settings, (a) i.i.d. case, (b) angle spread is 60 degrees, and (c) angle spread is 6 degrees, are plotted respectively.

(a) i.i.d. case

(b) angle spread is 60 degrees

31
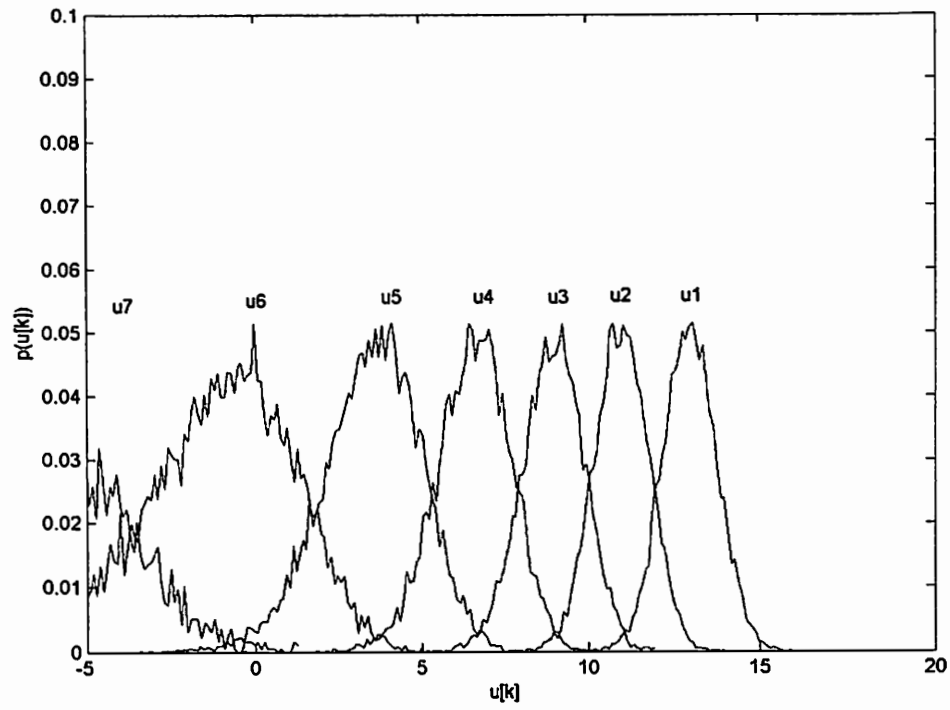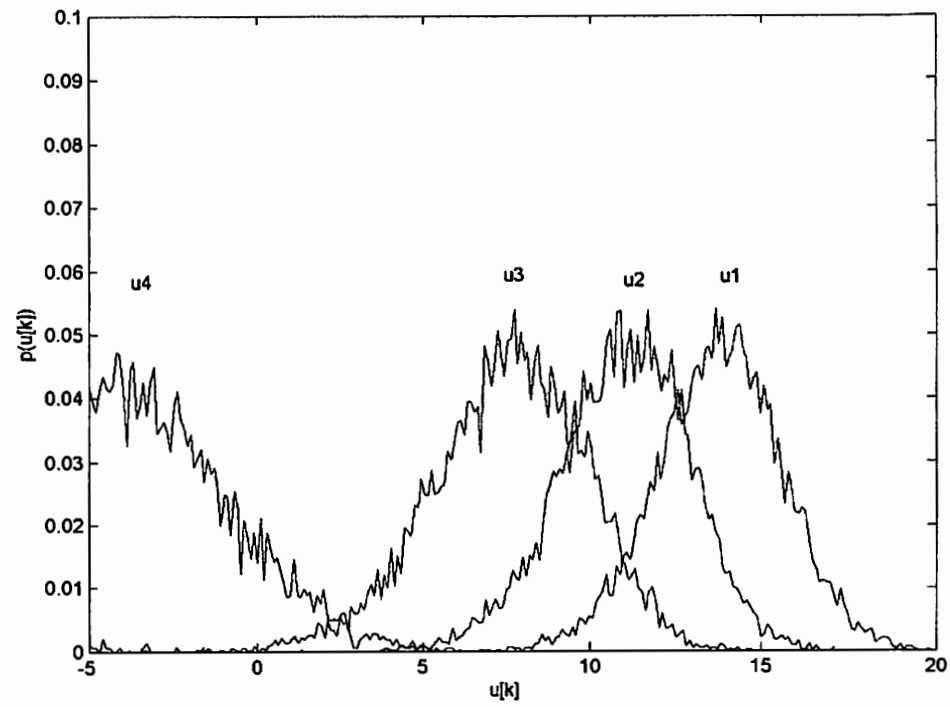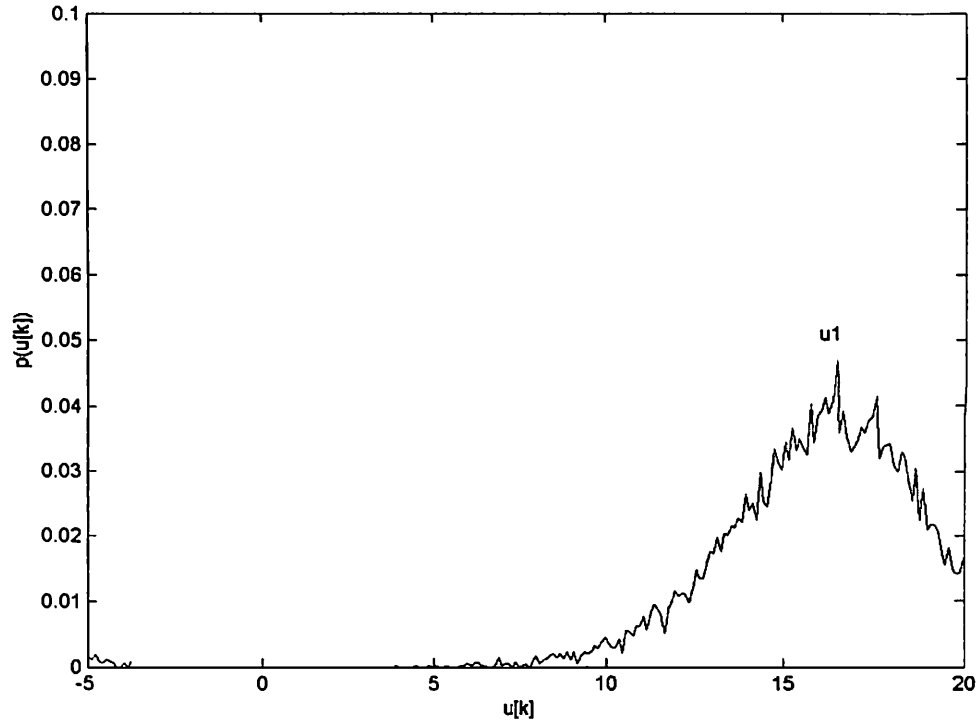
(c) angle spread is 6 degrees

Fig. 3.6 The PDF of the ordered eigenvalues of HH^+ under Rayleigh fading environment for hexagon antenna array deployed 7 by 7 MIMO system. The PDFs are normalized to have the same height for display purpose.

In Fig. 3.6, μ_1 is the largest eigenvalue and μ_7 is the smallest. As the angle spread decreases, the multiple channels become correlated to each other; the median of μ_1 increases slightly, but the median of $\mu_k, k \geq 2$, decreases. Another observation is that the disparity among those subchannels increases, which means that when the channels are deeply correlated, the subchannel with the largest eigenvalue becomes dominant.

C. The Optimal Power Allocation Strategy

If the receiver knows the instantaneous channel gain, i.e., the CSI, and feedbacks to the transmitter, the classical water-filling algorithm can be used to allocate the transmit power efficiently. This algorithm is regarded as the optimal power allocation strategy [22]. The basic idea of this algorithm is to allocate more transmit power on the channel corrupted by less noise and spend less power on bad channels. The equation for this can be given as [32]

$$D_S(i) = \left(\mu - \frac{1}{|D_H(i)|^2} \right)^+, \quad 1 \leq i \leq \min(M, N) \tag{3.18}$$

where μ is the water-fill level and satisfies $\sum_{i}^{\min(M,N)} D_S(i) = P_T$, and x^+ is defined as the

$\max(x, 0)$. Then the channel capacity for a single-user becomes

$$C = \sum_{i} (\log_2 (\mu |D_H(i)|^2))^+ \tag{3.19}$$

The performance comparison between equal power allocation and the optimal power allocation schemes is shown later.

3.1.5 Correlation Matrix Model

A. The Model Introduction

This model proposed by Gesbert [23] provides a more general equation to represent channel matrix H including several scenarios. It is supposed that there are S scatterers (typically $S > 10$ is sufficient) around the transmitter and receiver. The transmitter scatterers will relay the RF signals to the receiver scatterers, which can be regarded as an

array of virtual antennas or relay with large antenna spacing. The model is visualized in Fig. 3.7 [23].
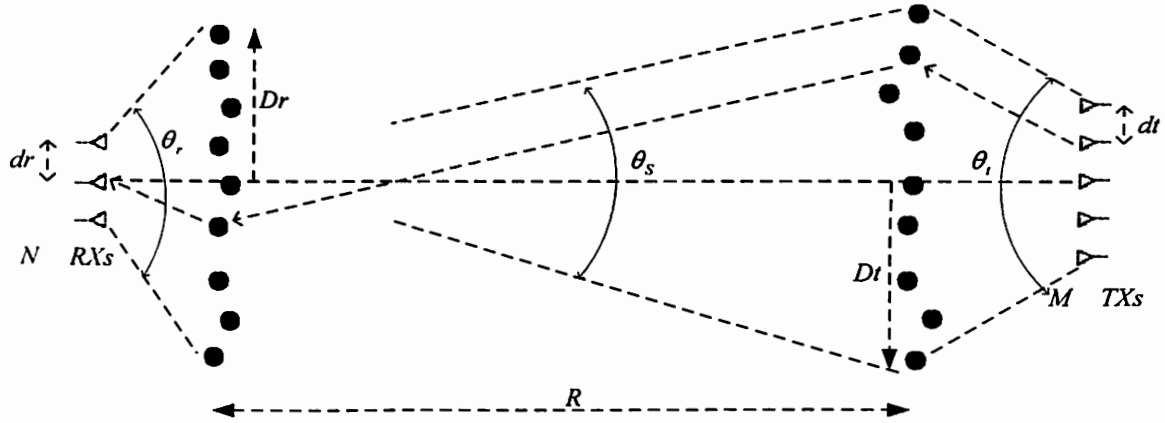
Fig. 3.7 Correlation matrix model with scatterers.

In Fig. 3.7, θ_t is the angle spread between the transmitter and its scatterers; θ_r is the angle spread between the receiver and its scatterers; θ_S is the angle spread from the transmitter scatterers to the receiver scatterers, while R is the distance between the transmitter scatterers and the receiver scatterers; and D_t and D_r are the radii of scatterers. We also assume the radius of scatterers is equal to the distance between the scatterers and antenna arrays. The terms d_r, d_t are the antenna spacing at the receiver and the transmitter, respectively. If scatterers are uniformly distributed, we can calculate the correlation between the two signal rays. The correlation between two receiver antennas m, and k can be given as [33]

$$R_{m,k} = \frac{1}{S} \sum_{l=-\frac{S-1}{2}}^{\frac{S-1}{2}} e^{-2\pi j(k-m)d_r \cos(\frac{\pi}{2}+\theta_{r,l})} \tag{3.20}$$

where S is the total number of receiver scatterers, $\theta_{r,i}$ is the angle spread of the i th scatterer. N receiver antennas can produce an $N \times N$ correlation matrix. From (3.20), we can verify that the correlation matrix is controlled by the antenna spacing d_r and angle spread θ_r. For large values of d_r and/or θ_r, correlation matrix will converge to the identity matrix, which gives uncorrelated fading; while small values of d_r and/or θ_r, make the correlation matrix fully correlated. This observation matches the conclusion in the one ring model.

Similarly, we can express the correlation matrix between the transmitter scatterers and receiver scatterers, and that between transmitters and their scatterers. Finally, the channel matrix can be written as the product of the square roots of several correlation matrixes and some Rayleigh fading factors [23]

$$H = \frac{1}{\sqrt{S}} R^{1/2}_{\theta_r,d_r} G_r R^{1/2}_{\theta_s,2D_r/S} G_t R^{1/2}_{\theta_t,d_t} \tag{3.21}$$

where $R^{1/2}_{\theta_r,d_r}$ is the $N \times N$ matrix controlling the receiver antenna correlation; G_r is the $N \times S$ i.i.d. Rayleigh fading matrix; $R^{1/2}_{\theta_s,2D_r/S}$ is the $S \times S$ matrix representing the characteristics of correlation between two sides of scatterers; G_t is the $S \times M$ i.i.d. Rayleigh fading matrix, and $R^{1/2}_{\theta_t,d_t}$ is the $M \times M$ matrix controlling the transmit antenna correlation. The term $\frac{1}{\sqrt{S}}$ is multiplied in front of the product such that the channel matrix is independent of the number of scatterers.

B. More Discussions

- The rank of $R^{1/2}_{\theta_S,2D_r/S}$ depends on the radius of scattering and distance between the transmitter scatterers and the receiver scatterers, not the transmitter or receiver antenna spacing.

- In the high rank region, $R^{1/2}_{\theta_S,2D_r/S}$ becomes a unitary matrix, the product $G_r G_t$ can converge to a single Rayleigh distributed matrix by using the central limit theorem. Thus, the channel matrix becomes $R^{1/2}_{\theta_r,d_r} H_w R^{1/2}_{\theta_t,d_t}$ where H_w represents a single Rayleigh matrix. If the fading is uncorrelated on both sides (i.e. $R^{1/2}_{\theta_r,d_r} = I_N$ and $R^{1/2}_{\theta_t,d_t} = I_M$), the MIMO channels become independent Rayleigh channels.

- In the low rank region, $R^{1/2}_{\theta_S,2D_r/S}$ becomes the all ones matrix, the channel matrix changes to $R^{1/2}_{\theta_r,d_r} G_r G_t R^{1/2}_{\theta_t,d_t}$. The channel capacity will drop down due to loss of multiplexing gain.

- The channel situation will vary between the above two cases depending on the angle spread and the antenna spacing.

From above discussions, we can see that equation (3.21) gives a simple but general expression of MIMO channels including several different situations. The simulation result of this model is shown in the Fig. 3.8.

In the simulation, there are 20 scatterers at the transmitter and receiver, respectively. Scatterers are perpendicular to the horizontal line. The distance R between transmitter and receiver scatterers is 10 km. We use $M = N = 3$ antennas on both sides and the wavelength is 0.15 m. The received SNR is 10 dB. Since we assume the radius of scatterers is equal to the distance between the scatterers and antenna arrays, the large

angle spread makes low correlation for $R_{\theta_r,d_r}^{1/2}$ and $R_{\theta_t,d_t}^{1/2}$. The channel average (mean)

capacity is mainly determined by the radius of scatterers.
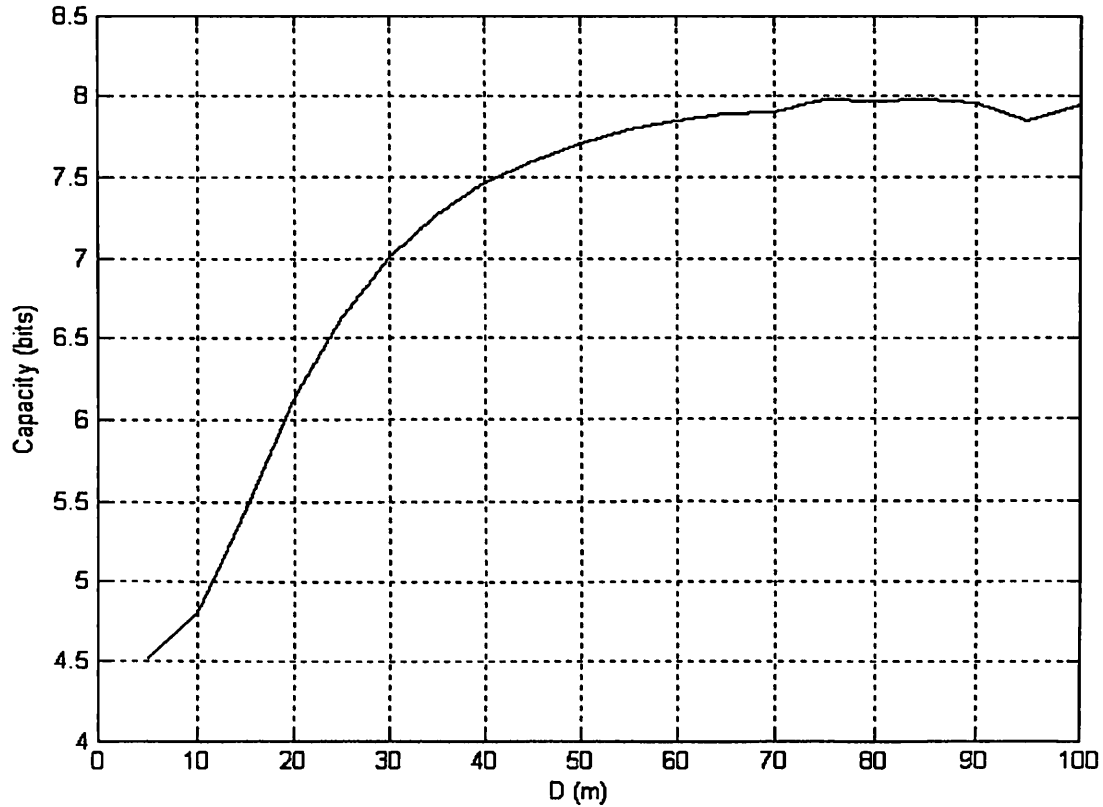
Fig. 3.8 Average capacity versus the radius of scatterers under only Rayleigh fading.

3.2 Macroscopic MIMO System

As introduced in the literature review, microdiversity and macrodiversity combining methods can be used to explore signal selection and signal combining, but none of the available papers give the capacity expression of the base station diversity MIMO scheme. And most MIMO papers just consider the Rayleigh fading, not the log-normal shadowing effect.

In this section, a macroscopic diversity combining (MDC) MIMO system is proposed, called the MIMO-MDC system. By deploying several base stations geographically separated to support one cell, the log-normal shadowing component can be mitigated and signals from different base stations can be combined to provide high data rate. The three base stations deployed macroscopic MIMO system architecture is shown in Fig. 3.9.
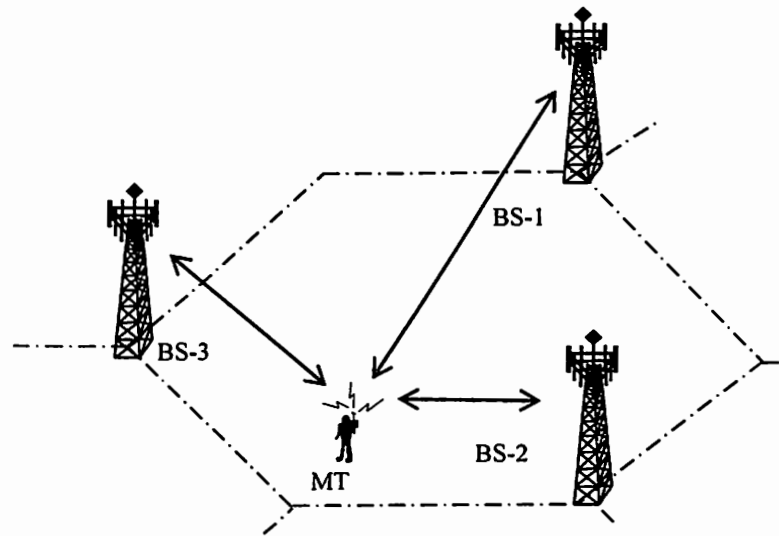
Fig. 3.9 An illustration of a MIMO-MDC system architecture with $M = 3$.

3.2.1 System Model and Capacity Equation

A. i.i.d. Fading Channel Case

In this thesis, different base stations are considered with the same number of antennas M. Antennas at one base station are far enough such that the signals from the same base stations are uncorrelated. Therefore the Rayleigh fading components from those signals are independent. Since the log-normal shadowing component is a large-

scale fading, it is assumed to be the same for the signals from the same base station. The one ring model is still used as a propagation model. For a non-macroscopic one base station MIMO system, equation (3.2) is rewritten for convenience

$$C = E_H[\log_2 |I_N + HQH^+|]$$
(3.22)

where $H = H_R \omega^{1/2}$. H_R is the Rayleigh fading channel matrix and $\omega^{1/2}$ is the common log-normal shadowing factor. For the macroscopic MIMO system, the channel matrix $\widetilde{H} = \widetilde{H}_R \Omega^{1/2}$, where $\widetilde{H}_R = [H_1 \quad H_2 \quad \dots \quad H_L]$, L is the number of macroscopic base stations participating in the communication, and H_i is a $N \times M$ matrix whose elements are i.i.d. complex Rayleigh distributed random variables. The log-normal shadowing component is changed to

$$\Omega^{1/2} = \begin{bmatrix} \omega_1^{1/2} I_M & & & \\ & \omega_2^{1/2} I_M & & \\ & & \ddots & \\ & & & \omega_L^{1/2} I_M \end{bmatrix}$$
(3.23)

where $\omega_i^{1/2}$ is the log-normal random variable of the i th base station to the mobile user and I_M is the $M \times M$ unit matrix. Since the total transmit power of the macroscopic MIMO system is the same as the non-macroscopic MIMO system and if the power is allocated equally to all base stations, the equation (3.22) becomes

$$C = E_H \left[\log_2 \left| I_N + \frac{\widetilde{H}Q\widetilde{H}^+}{L} \right| \right]$$
(3.24)

B. Correlation Case

In a typical cellular mobile communication system, the fading channels usually are not independent, and then the model in [23] can be used. Since the antennas at the base station are much higher than that at the mobile site, the scatterers at the transmitter side are not considered, and the one ring model is employed. In many cases, since there are ample local scatterers at the mobile site, the correlation at the receiver side is very small if we consider the downlink. For the sake of simplicity, we assume $R_{\theta_r,d_r}^{1/2} = I$ in (3.21), i.e., there is no correlation at the receiver side. Finally, the channel matrix from the ith base station to the receiver is reduced to

$$H_i = \frac{1}{\sqrt{S}} H_w R_{\theta_i,d_i}^{1/2} \qquad (3.25)$$

where H_w is the complex i.i.d. Rayleigh random matrix and $R_{\theta_i,d_i}^{1/2}$ is the correlation matrix between the transmitter and the scatterers around receiver. The capacity of the whole macroscopic system still follows (3.24).

3.2.2 Performance Simulation of MIMO-MDC System

In the simulation, there are three antennas at the mobile user and each base station. One to four combining base stations is considered respectively. Since there is enough space to deploy antennas away from each other, the distance between adjacent antennas is 3 times the wavelength. This means that the transmitted signals are independent. The wavelength is 0.15 m. There are 20 scatterers and the radius of the scatterer circle is 30 m. The average SNR is 17 dB, the standard deviation of the log-normal shadowing part is 8 dB and that of Rayleigh fading is 0.5 dB.

40

In real wireless communication systems, sometimes the duration of the transmitted signal is much less than the channel variability. This is true for burst data communication systems. In this case, the average capacity can not be applied. Instead of using average capacity, we use the outage capacity to evaluate the system performance. It also can give an insight of minimum data rate provided to a majority of people or a covered region. 10% outage capacity is used in this section to evaluate the system performance as given in (2.14). The capacities of MIMO-MDC system with different number of combining base stations at 10% outage are plotted versus different angle spread in Fig. 3.10. The equal power allocation strategy and the optimal power strategy are used separately to show the difference.
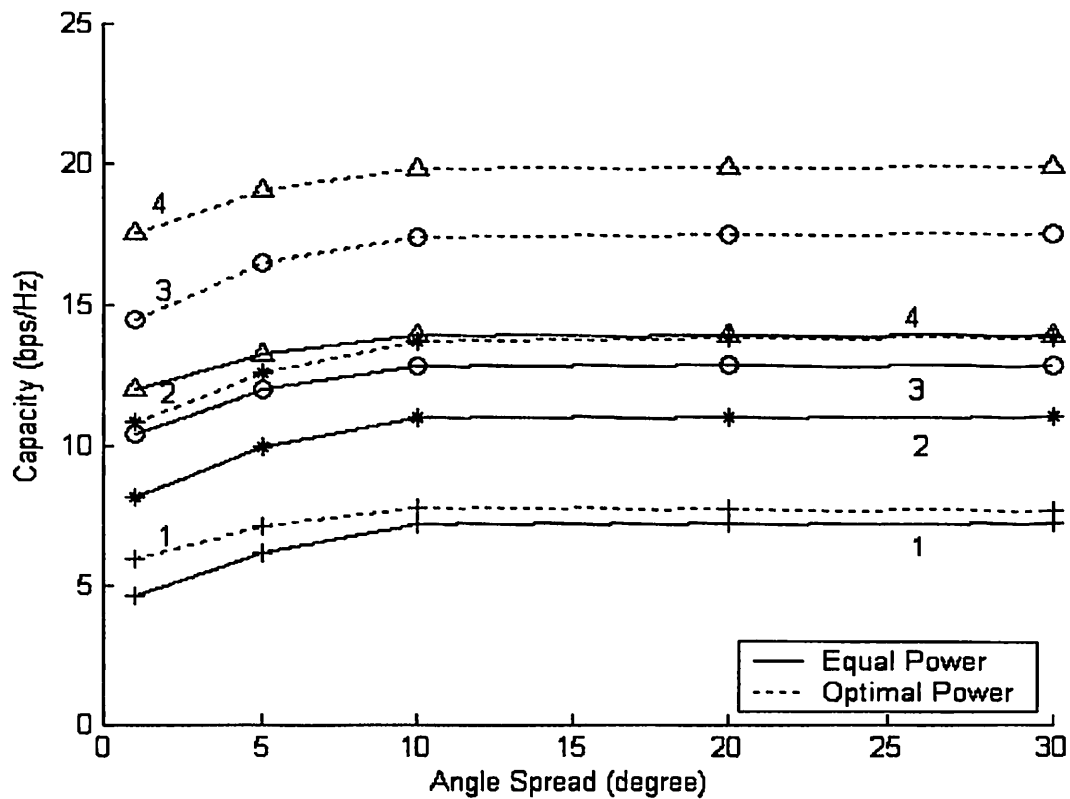
Fig. 3.10 Capacities of MIMO-MDC system with 1, 2, 3 and 4 combining base stations respectively at 10% outage under composite fading environment.

The cumulative distribution functions (CDF) of three different topologies of MIMO systems with 10 degree angle spread are simulated. The first scheme is the non-macroscopic 3 by 3 MIMO systems; the second one is the non-macroscopic 9 by 9 MIMO systems and the last one is the proposed 3 base stations MIMO-MDC system with 9 antennas at the receiver site. Therefore, in the MIMO-MDC system, the total number of transmit antennas is 9 and equal to that of 9 by 9 MIMO system. The simulation results for the i.i.d. fading case, equal power strategy and the optimal power strategy are plotted in Fig. 3.11 respectively.
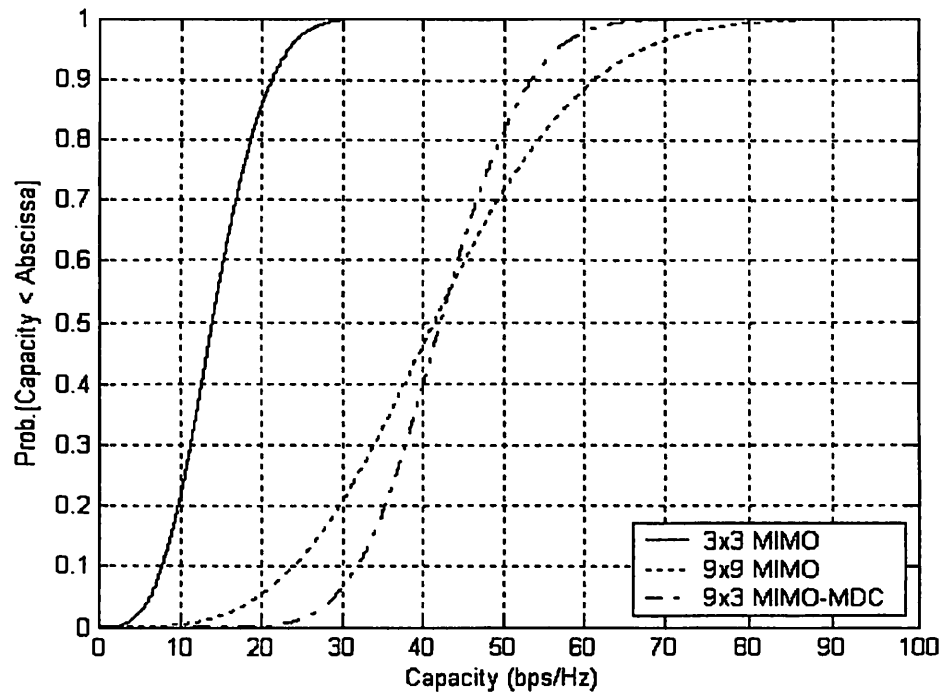
(a) i.i.d. fading
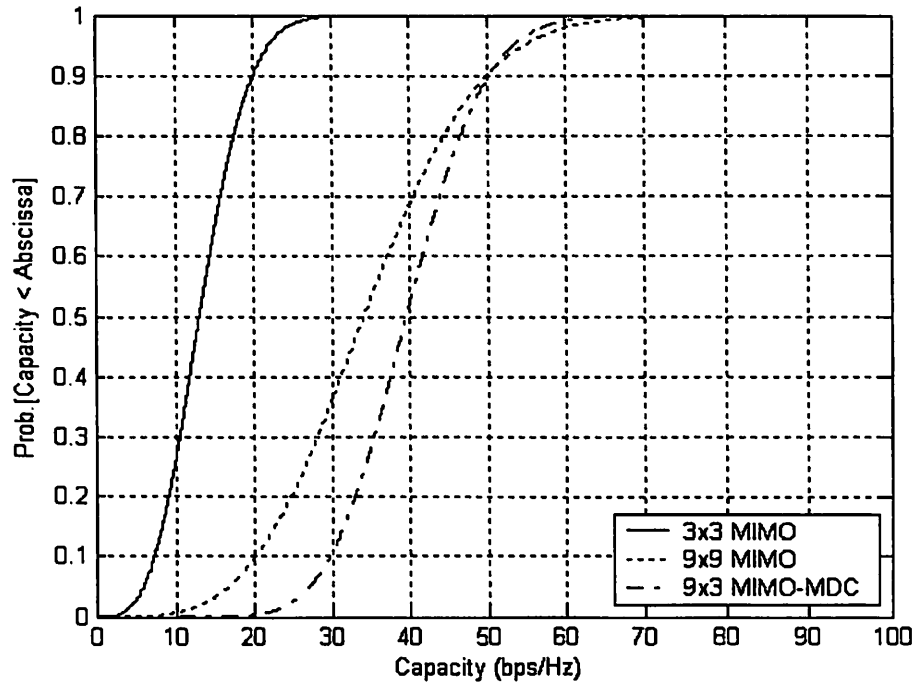
(b) 10 degree angle spread with equal transmit power strategy
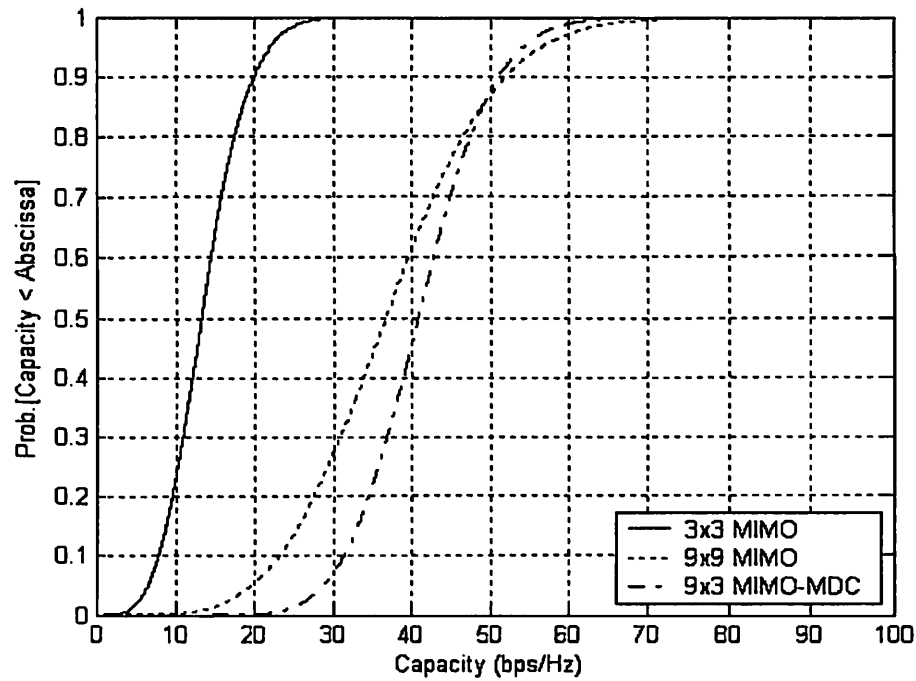
(c) 10 degree angle spread with the optimal power strategy

Fig. 3.11 The CDF of three MIMO systems under composite fading environment.

3.2.3 Observations and Discussions

In Fig. 3.10, the solid lines are capacity curves of equal power strategy, while the dashed lines are capacity curves of the optimal power strategy (i.e., water-filling solution). From the figure, it is shown that the capacity of four combining base stations is almost double the capacity for a single base station MIMO system with the equal power strategy. The capacity of the optimal power strategy is much larger than that of the equal power strategy, especially when the macroscopic base station combining scheme is used. The capacity of four combining base stations with the optimal power strategy is almost three times the capacity for a single base station MIMO system.

Fig. 3.11 compares three MIMO system topologies under i.i.d. fading case, 10 degree angle spread with equal power strategy and 10 degree angle spread with the optimal power strategy. The most important observation is that although the MIMO-MDC system has the same number of transmit antennas as the 9 by 9 non-macroscopic MIMO system, it has almost 10 bps/Hz improvement above that of 9 by 9 MIMO system when the 10% outage capacity is considered. Comparing the performance between (b) and (c), the optimal power strategy provides better outage capacity than that of the equal power strategy, which means the capacity of the optimal strategy is closer to that of the i.i.d. case.

As verified by the simulations, the MIMO-MDC system can maximize the spatial multiplexing gain while combating the Rayleigh fading by deploying multiple antennas at the receiver and mitigating the log-normal shadowing effect by combining independent signals from different base stations. The optimal power strategy can give extra performance improvement compared to the equal power strategy. But the disadvantage of

44

the optimal power strategy is that it needs the instantaneous CSI feedback to the transmitter. This is not easily obtainable when the channel fluctuates very fast or the mobile user moves fast. Considering this reason, the equal power strategy is easier to implement and more practical.

Chapter 4

Adaptive Modulation in Macroscopic Diversity System

In this Chapter, Adaptive modulation technology applications based on four different constraints under Rayleigh fading and composite fading environments are illustrated. The adaptive modulation scheme combined with macroscopic diversity technique is proposed in section 4.2. The spectral efficiency performance of the adaptive macroscopic selection diversity scheme and the adaptive macroscopic MRC scheme is then compared.

4.1 Adaptive Modulation Technology

As explained in Chapter 3, the nature of the wireless channel varies with time. Sometimes the channel condition is good, which means there is not much influence of attenuation or fading factors, but sometimes the channel experiences deep fading. Such a variation in the channel condition also affects the SNR. When the instantaneous SNR is small, fixing of the transmission data rate or modulation constellation will deteriorate the system performance. Thus, if a system can transmit data adaptively based on the channel variation, it will work very efficiently or optimally. Such a system can maximize the data rate and satisfy the QoS at the same time.

4.1.1 Adaptive Modulation Study

As mentioned in [5], several parameters such as the transmit power, constellation size, BER, coding scheme or any combination of those parameters can be varied to optimize the system. Considering transmission power, constellation size and BER in transmission, [5] investigates adaptive modulation based on four cases only in the Rayleigh fading environment: continuous rate with an average BER constraint (C-Rate A-BER), continuous rate with an instantaneous BER constraint (C-Rate I-BER), discrete rate with an average BER constraint (D-Rate A-BER), and discrete rate with an instantaneous BER constraint (D-Rate I-BER). In modern wireless applications, especially in multimedia transmissions, the instantaneous BER constraint is more crucial. Since C-Rate A-BER gives the optimal output, only three of those schemes are demonstrated in this study namely C-Rate A-BER, C-Rate I-BER and D-Rate I-BER. Different QAM constellations used on the different channels are 4QAM, 16QAM, 64QAM, 256QAM, 1024QAM, and 4096QAM for the discrete rate case. The effect of channel coding is not considered.

A. System Model and Constraint Expression

The system model and notation follows that of [5]. The model illustration is shown in Fig. 4.1.

TRANSMITTER

CHANNEL

$\sqrt{g[i]}$ $n[i]$

RECEIVER

Demodulation and decoding

$\hat{r}[i]$

$r[i]$

Adaptive modulation and coding

Power control $S[i]$

$x[i]$

$\times$

$+$

$y[i]$

Channel estimator

$\hat{g}[i]$

$\hat{g}[i]$

$\hat{g}[i]$
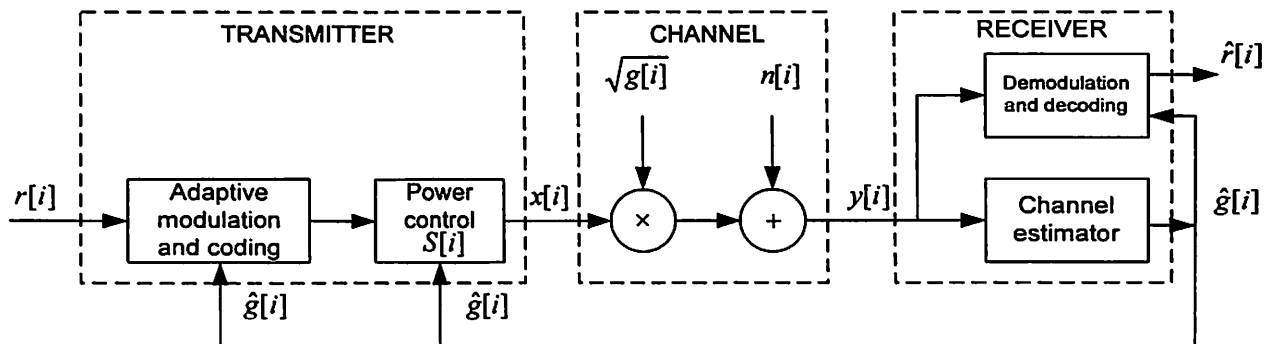
Fig. 4.1 Adaptive modulation system model.

In Fig. 4.1, $g[i]$ is the channel power gain, $n[i]$ is the additive white noise and i is the time index. The most important issue in this model is that the feedback channel from the receiver to the transmitter should be fast and accurate. Therefore, another assumption made is the feedback channel exhibits no error and delay. In other words, $\hat{g}[i] = g[i]$, where $g[i]$ is the channel power gain and $\hat{g}[i]$ is the estimated channel gain at the receiver. Since the transmit power can be adjusted based on the instantaneous SNR, it is denoted as $S(\gamma[i])$. When the channel condition deteriorates severely, the transmit power is being saved and the saved power is used when the channel is in good condition.

Like in [5], the spectral efficiency equals the average data rate per unit bandwidth. For the continuous rate case, it can be expressed as

$$C_c = \int_0^\infty k(\gamma)p(\gamma)d\gamma \quad \text{bps/Hz} \tag{4.1}$$

$p(\gamma)$ is the PDF of instantaneous SNR γ and $k(\gamma)$ represents how many bits per symbol can be transmitted with the corresponding γ. The rate adaptation $k(\gamma)$ is limited by the average transmit power $\overline{S}$ and the BER constraint (average BER or instantaneous BER). The average transmit power constraint is

$$\int_0^\infty S(\gamma)p(\gamma)d\gamma \le \overline{S} \tag{4.2}$$

When BER is considered, instantaneous BER constraint means the system must satisfy a constant BER all the time, i.e., $\overline{BER} = BER(\gamma)$. It is a more strict condition than the average BER constraint. The latter one can be expressed as

$$\overline{BER} = \frac{\int_0^\infty BER(\gamma)k(\gamma)p(\gamma)d\gamma}{\int_0^\infty k(\gamma)p(\gamma)d\gamma} \tag{4.3}$$

For discrete rate adaptation, the spectral efficiency is given by

$$C_d = \sum_{i=0}^{N-1} k_i \int_{\gamma_i}^{\gamma_{i+1}} p(\gamma)d\gamma \quad \text{bps/Hz} \tag{4.4}$$

where N is the number of available constellations. And the average BER becomes

$$\overline{BER} = \frac{\sum_{i=0}^{N-1} k_i \int_{\gamma_i}^{\gamma_{i+1}} BER(\gamma)p(\gamma)d\gamma}{\sum_{i=0}^{N-1} k_i \int_{\gamma_i}^{\gamma_{i+1}} p(\gamma)d\gamma} \tag{4.5}$$

For M-QAM system, the $BER(\gamma)$ in (4.3) and (4.5) can be approximated as [5]

$$BER(\gamma) \approx c_1 \exp\left[\frac{-c_2\gamma\dfrac{S(\gamma)}{\overline{S}}}{f(k(\gamma))}\right] \tag{4.6}$$

where

$$f(k(\gamma)) = 2^{c_3 k(\gamma)} - c_4 \tag{4.7}$$

and c_1, c_2, c_3, c_4 are positive fixed constants used to give a good approximation for BER. They are given as $c_1 = 0.2, c_2 = 1.6, c_3 = c_4 = 1$ [5]. The equations for different constraint cases are given as the following. The derivations of those equations are presented in Appendix A.

49

B. Equations for C-Rate A-BER

From [5], it is known that the Lagrange method can be used to solve this optimization problem. The Lagrange equation constrained by (4.2) and (4.3) is

$$J(k(\gamma), S(\gamma)) = \int_0^\infty k(\gamma)p(\gamma)d\gamma + \lambda_1[\int_0^\infty BER(\gamma)k(\gamma)p(\gamma)d\gamma - \overline{BER} \int_0^\infty k(\gamma)p(\gamma)d\gamma]$$
$$+ \lambda_2[\int_0^\infty S(\gamma)p(\gamma)d\gamma - \overline{S}]$$

(4.8)

The optimal rate and power adaptation should satisfy

$$\frac{\partial J}{\partial k(\gamma)} = 0 \text{ and } \frac{\partial J}{\partial S(\gamma)} = 0$$

(4.9)

By using the BER expression in (4.6) and solving (4.9), the power and BER adaptation that maximize the spectral efficiency satisfy

$$\frac{S(\gamma)}{\overline{S}} = \max\left[\frac{f(k(\gamma))}{\frac{\partial f(k(\gamma))}{\partial k(\gamma)} \lambda_2 \overline{S}}(\lambda_1 \overline{BER} - 1) - \frac{f(k(\gamma))^2}{c_2\gamma \frac{\partial f(k(\gamma))}{\partial k(\gamma)} k(\gamma)}, 0 \right]$$

(4.10)

for nonnegative $k(\gamma)$, and

$$BER \ (\gamma) = \frac{\lambda_2 \overline{S} f(k(\gamma))}{\lambda_1 c_2 \gamma k(\gamma)}$$

(4.11)

where $\frac{S(\gamma)}{\overline{S}}$ is the ratio between instantaneous transmit power and the average power.

The rate adaptation $k(\gamma)$ is either zero or the nonnegative solution of

$$\frac{\lambda_1 \overline{BER} - 1}{\frac{\partial f(k(\gamma))}{\partial k(\gamma)} \lambda_2 \overline{S}} - \frac{f(k(\gamma))}{c_2\gamma \frac{\partial f(k(\gamma))}{\partial k(\gamma)} k(\gamma)} = \frac{1}{\gamma c_2} \ln\left[\frac{\lambda_1 c_1 c_2 \gamma k(\gamma)}{\lambda_2 \overline{S} f(k(\gamma))} \right]$$

(4.12)

50

C. Equations for C-Rate I-BER

The instantaneous BER constraint is $BER(\gamma) = \overline{BER}$, and then by inverting (4.6),

$k(\gamma)$ can be expressed as a function of adaptive power $S(\gamma)$ and the fixed bit error rate

$$k(\gamma) = \begin{cases} \dfrac{1}{c_3} \log_2 \left[c_4 - \dfrac{c_2 \gamma}{\ln(\frac{\overline{BER}}{c_1})} \dfrac{S(\gamma)}{\overline{S}} \right], & S(\gamma) \geq 0, k(\gamma) \geq 0 \\ 0 & else \end{cases} \qquad (4.13)$$

The Lagrange equation for this case is [5]

$$J(S(\gamma)) = \int_0^\infty k(\gamma)p(\gamma)d\gamma + \lambda[\int_0^\infty S(\gamma)p(\gamma)d\gamma - \overline{S}] \qquad (4.14)$$

The optimal power adaptation must satisfy

$$\dfrac{\partial J}{\partial S(\gamma)} = 0, \quad S(\gamma) \geq 0, \quad k(\gamma) \geq 0 \qquad (4.15)$$

Replacing $k(\gamma)$ with (4.13) and solving (4.15), the optimal power ratio is given by

$$\dfrac{S(\gamma)}{\overline{S}} = \begin{cases} \dfrac{1}{\gamma_0 K} - \dfrac{1}{\gamma K}, & S(\gamma) \geq 0 \\ 0 & else \end{cases} \qquad (4.16)$$

where $\gamma_0 \geq 0$ is the cutoff fade depth that can be obtained by substituting (4.16) in (4.2)

and solving the following equation

$$\int_{\gamma_0}^\infty \dfrac{1}{K} \left[\dfrac{1}{\gamma_0} - \dfrac{1}{\gamma} \right] p(\gamma)dr = 1 \qquad (4.17)$$

in which K is given as

$$K = - \dfrac{c_2}{c_4 \ln\left(\dfrac{\overline{BER}}{c_1} \right)} \qquad (4.18)$$

When the channel is extremely distorted and the instantaneous SNR is less than the cutoff

fade γ_0, increase in transmit power is of no use. Rather, in applications that permit, we

can save the same power and allocate it to the channel when it is in good condition so that we can apply a larger QAM constellation size and increase the data rate still satisfying the fixed BER.

D. Equations for D-Rate I-BER

In reference to [5], the transmission rate is assumed to be selected from the set $\{k_i\}_{i=0}^{N-1} = \{0\ 2\ 4\ 6\ 8\ 10\ 12\}$, which means $N=7$. The same rate k_i is assigned when the instantaneous SNR is in the region $[\gamma_i, \gamma_{i+1})$. The Lagrange method is still applied to find the optimal region boundaries that maximize spectral efficiency. The equation is

$$J(\gamma_i) = \sum_{0 \le i \le N-1} k_i \int_{\gamma_i}^{\gamma_{i+1}} p(\gamma)d\gamma + \lambda \left[\sum_{0 \le i \le N-1} \int_{\gamma_i}^{\gamma_{i+1}} \frac{h(k_i)}{\gamma} p(\gamma)d\gamma - 1 \right] \qquad (4.19)$$

where $h(k_i) = -(1/c_2)\ln(\overline{BER}/c_1)f(k_i)$, and $f(k_i) = 2^{k_i} - 1$. By solving

$$\frac{\partial J}{\partial \gamma_i} = 0, \qquad 0 \le i \le N-1 \qquad (4.20)$$

the optimal rate region boundaries are given as

$$\gamma_i = \begin{cases} \dfrac{h(k_0)}{k_0}\rho, & i = 0 \\[2mm] \dfrac{h(k_i) - h(k_{i-1})}{k_i - k_{i-1}}\rho, & 1 \le i \le N-1 \end{cases} \qquad (4.21)$$

In (4.21), ρ is determined by the average power constraint (4.2).

52

E. Numerical Search and Results

To find the optimal parameter in the Lagrange equation, the bisection method is used. Bisection search method is a fast convergent algorithm to find the value for the parameter to make the equation equal to zero [34]. The basic one-dimensional bisection method is used in C-Rate I-BER and D-Rate I-BER case, while for the C-Rate A-BER case a two-dimensional bisection is applied. Since the C-Rate A-BER case is more complex, only the two-dimensional bisection method is explained in more detail.

1) Two-dimensional bisection numerical search

In order to make (4.10) and (4.11) satisfy constraints (4.2) and (4.3) at the same time, for any fixed λ_1 and $\lambda_2 \bar{S}$, we can find $k(\gamma)$ over all γ that satisfies (4.12). The function of $k(\gamma)$ will be zero if $k(\gamma) \geq 0$ and $S(\gamma) \geq 0$ are not satisfied. Taking the value of $k(\gamma)$ back to (4.10) and (4.11), we obtain $\dfrac{S(\gamma)}{\bar{S}}$ and $BER(\gamma)$ in terms of $k(\gamma)$. A two-dimensional search method is applied to find λ_1 and $\lambda_2 \bar{S}$ that make $\dfrac{S(\gamma)}{\bar{S}}$ and $BER(\gamma)$ satisfy the average power constraint (4.2) and the average BER constraint (4.3). The real power constraint and the BER constraint that would be tested are:

$$\int_0^\infty \frac{S(\gamma)}{\bar{S}} p(\gamma) d\gamma - 1 = 0 \tag{4.22}$$

$$\int_0^\infty BER(\gamma)k(\gamma)p(\gamma)d\gamma - \overline{BER}\int_0^\infty k(\gamma)p(\gamma)d\gamma = 0 \tag{4.23}$$

Initially, we consider λ_1 and $\lambda_2 \bar{S}$ to represent two orthogonal axes in a plane named as λ plane. If we want to find a fixed λ_1 and $\lambda_2 \bar{S}$ that satisfies (4.22) and (4.23),

mathematically we need to perform a two-dimensional search to find a crossing point of two curves. Those two curves are in λ plane to satisfy the power constraint and the average BER constraint separately.

In the algorithm, it is defined that the curves satisfy the power constraint as F1, F2 for BER constraint. It is also assumed that F1 and F2 are monotonically increasing or decreasing with reference to λ_1 and $\lambda_2 \bar{S}$. The bisection method is an efficient algorithm to find the root of a monotonic function, therefore in this research we perform a two-dimensional bisection search based on the sign change of F1 and F2.

As known, a plane could be divided into four parts if two monotonic curves in this plane cross each other. These two functions have different signs in these four parts, such as (+, +), (+, -), (-, +), and (-, -). Firstly, we choose four points on λ plane. Each point is located in one of these four regions. Such four points consist of a quadrilateral and guarantee that the desired point, which makes F1 and F2 zeros, is in this area. Two monotonic curves divide the λ plane and have different signs as shown in Fig 4.2.
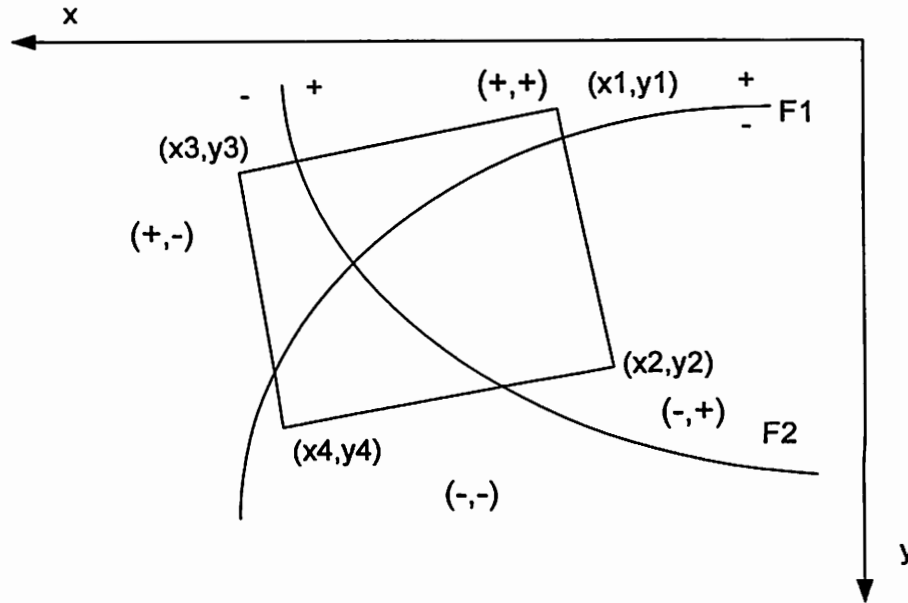
Fig. 4.2 Four regions on the λ plane divided by two monotonic curves from the two-dimensional bisection method.

In this case, x axis represents λ_1 and y axis represents $\lambda_2 \bar{S}$. As shown in the figure, the part below the F1 curve makes the power constraint have negative value; the upper part makes the power constraint have positive value. Likewise, the part below F2 curve makes the average BER constraint have a negative value; the upper part makes the average BER constraint have a positive value. The sign changes are also shown in the figure. The first sign in every bracket represents the sign for F1, and the second one represents the sign for F2. Finally, four points (x1, y1), (x2, y2), (x3, y3), and (x4, y4) are chosen, each one is chosen from a different region. Such a quadrilateral can guarantee that the desired point is in this rectangle. Then the bisection method is used to reduce the region and approach the desired point. The flow chart is as follows:
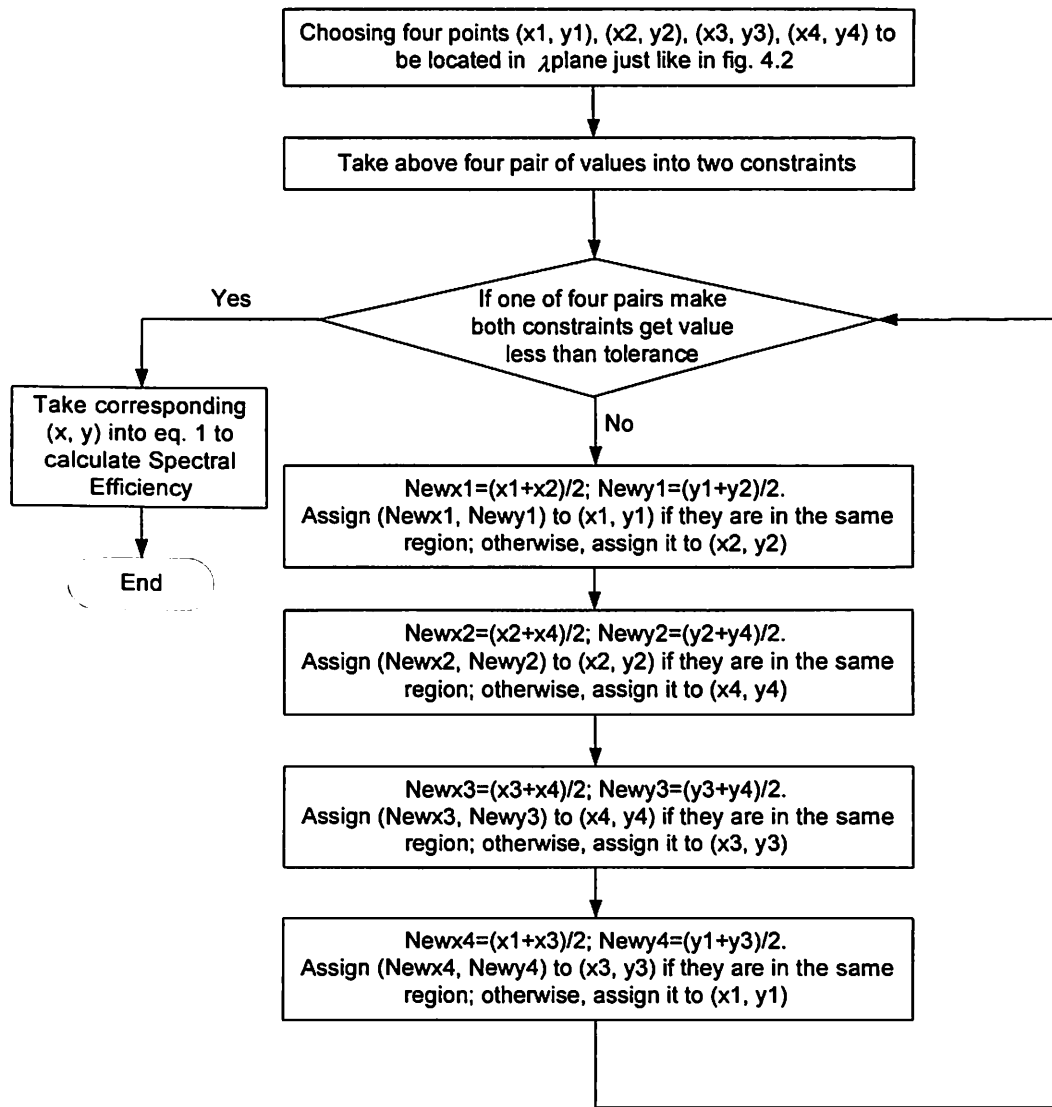
Fig. 4.3 Flow chart of the two-dimensional bisection method.

2) Numerical result

Based on the above two-dimensional bisection method and an easier one-dimensional bisection method, the mean spectral efficiency of the three different constraint cases with BER at 10^{-3} under Rayleigh fading environment are shown in the following figure.

Fig. 4.4 Mean spectral efficiency of the three different constraint cases with BER at 10^{-3} under the Rayleigh fading environment.

4.1.2 Adaptive Modulation under Composite Fading Environment

In [28], the PDF of the log-normal component expressed in dB is

$$p(\Gamma_0) = \frac{10}{\sigma \Gamma_0 \ln(10)\sqrt{2\pi}} \exp\left[-\frac{(10\log_{10}\Gamma_0 - m)^2}{2\sigma^2} \right] \qquad (4.24)$$

where m and σ are the respective mean and standard deviation in dB of the log-normal component. Γ_0 is the local mean of fading. As introduced in Chapter 2, for the composite fading case, the Rayleigh component fluctuates fast on the log-normal variable. Then the PDF of composite fading can be represented as

$$p(\gamma) = \int_0^\infty \frac{10}{\sigma \Gamma_0^2 \ln(10)\sqrt{2\pi}} \exp\left(-\frac{\gamma}{\Gamma_0}\right) \cdot \exp\left[-\frac{(10\log_{10}\Gamma_0 - m)^2}{2\sigma^2}\right] d\Gamma_0 \qquad (4.25)$$

Unfortunately, there is no closed-form solution for the above equation. As in [29], a new log-normal distributed variable is used to approximate the composite fading variable. The PDF of the composite fading signal is

$$p(\gamma) \approx \frac{10}{\sigma_{an}\gamma \ln(10)\sqrt{2\pi}} \cdot \exp\left[-\frac{(10\log_{10}\gamma - \overline{\gamma}_{an})^2}{2\sigma_{an}^2}\right] \qquad (4.26)$$

where $\overline{\gamma}_{an}$ and σ_{an} are the approximated mean and the standard deviation of the logarithm of the log-normal component of this channel , i.e. $10\log_{10}\gamma$, respectively. The approximated $\overline{\gamma}_{an}$ and σ_{an} are equal to

$$\overline{\gamma}_{an} = \overline{\gamma} - 2.5 \quad dB \qquad (4.27)$$

$$\sigma_{an} = \sqrt{\sigma_\gamma^2 + 5.57^2} \quad dB \qquad (4.28)$$

where $\overline{\gamma}$ and σ_γ^2 are the exact mean and standard deviation of the log-normal component of that channel. This approximation is accurate if σ_γ^2 is greater than 6 dB [29]. In the simulation, σ_γ is set to 9 dB, $\overline{\gamma}$ is chosen from 5 dB to 30 dB.

Using the approximated PDF in the section 4.1.1, the mean spectral efficiency of adaptive modulation system under composite fading environment for the three constraint cases can be obtained as shown in Fig. 4.5
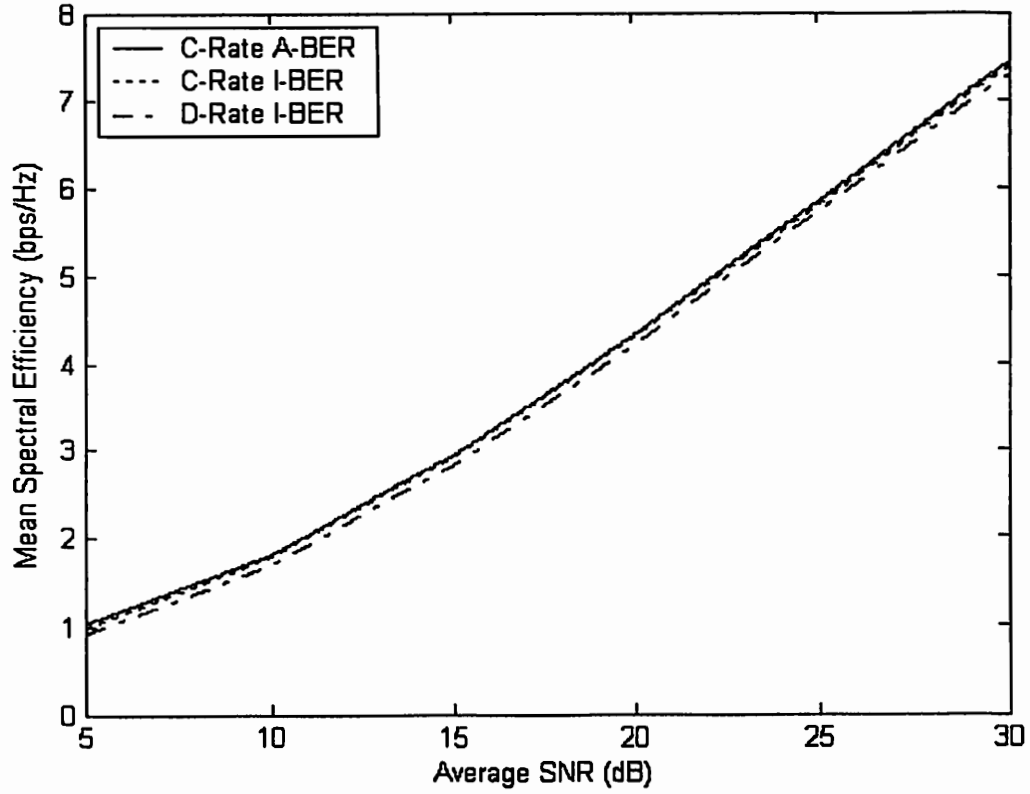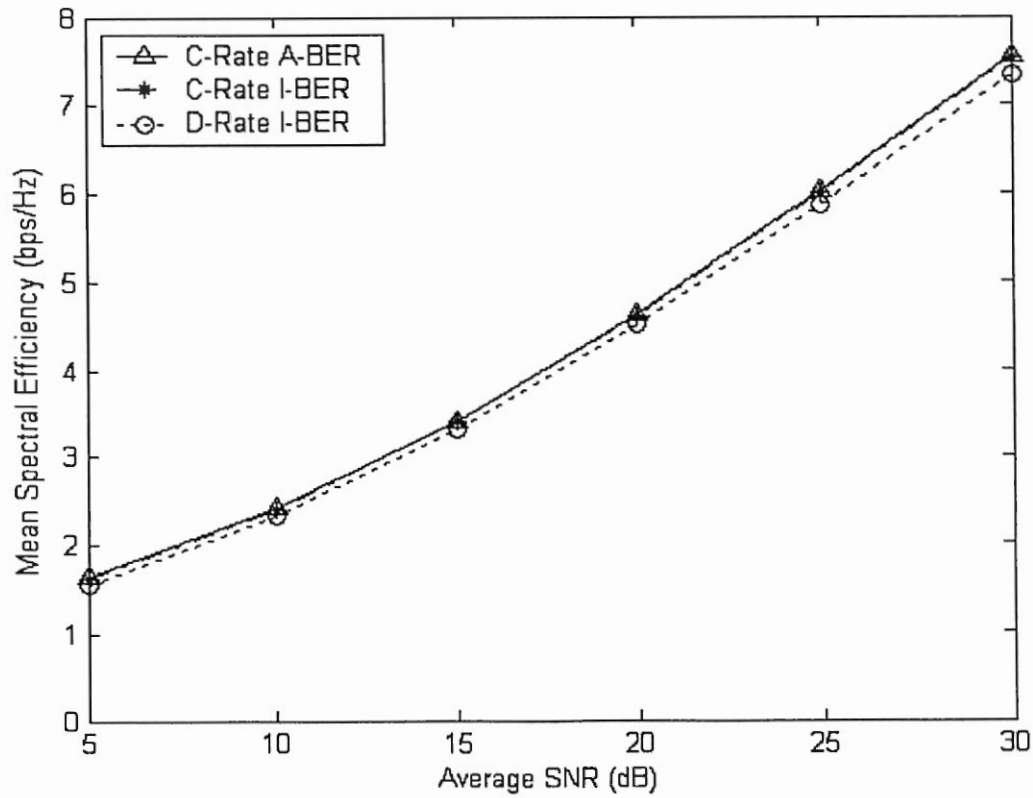
Fig. 4.5 Mean spectral efficiency of the three different constraint cases with BER at 10^{-3} under the composite fading environment.

4.2 Adaptive Macroscopic Diversity Schemes

In this section, the proposed adaptive macroscopic diversity systems are introduced. In the analysis model three base stations are deployed to support one single cell and each base station has only one antenna. The assumption results in mobile users in this cell to receive three uncorrelated Rayleigh plus log-normal signals. The transmission power is assumed to be adjusted based on the user location such that its local mean power remains the same regardless of the physical user location. In order to simplify the system, the BER of each independent channel is the same. Two adaptive macroscopic diversity

schemes are introduced. To start with, the spectral efficiency of the macroscopic selection diversity system under composite fading environment with C-Rate I-BER constraint is analyzed. The performance improvement is compared with that of a single base station system. Then in order to show the spectral efficiency of a macroscopic MRC system, a suboptimal case, which fixes the transmit power for each transmission, is introduced and compared to the optimal case. Finally, the spectral efficiencies of two adaptive macroscopic diversity systems are produced.

4.2.1 Adaptive Macroscopic Selection Diversity Scheme

In a rich fading environment consisting of Rayleigh fading plus log-normal fading, based on the feedback channel information, we select the base station whose channel has the highest SNR compared to other base stations. In order to simplify the model, as in [29], the mean and the standard deviation of signals from all base stations are assumed to be the same. Then the PDF of M-branch macroscopic selective diversity system is [28]

$$p(\gamma) = \frac{10M}{\sigma_{an}\gamma \ln(10)\sqrt{2\pi}} \cdot \exp\left[-\frac{(10\log_{10}\gamma - \overline{\gamma}_{an})^2}{2\sigma_{an}^2}\right] \cdot F\left[\frac{10\log_{10}\gamma - \overline{\gamma}_{an}}{\sigma_{an}}\right]^{M-1} \quad (4.29)$$

where $F[\cdot]$ is the cumulative normal distribution function, M is the number of base stations to support a single cell. Once the PDF of SNR is known, we can adaptively allocate the transmit power based on the channel condition and the fixed target BER. Taking the above PDF back to the equation for the C-Rate I-BER constraint, the spectral efficiency of adaptively modulated macroscopic selection diversity scheme can be obtained. The mean spectral efficiency comparison between the macroscopic selection diversity and a single base station for C-Rate I-BER case at the target BER of 10^{-3} is

presented in Fig. 4.6.
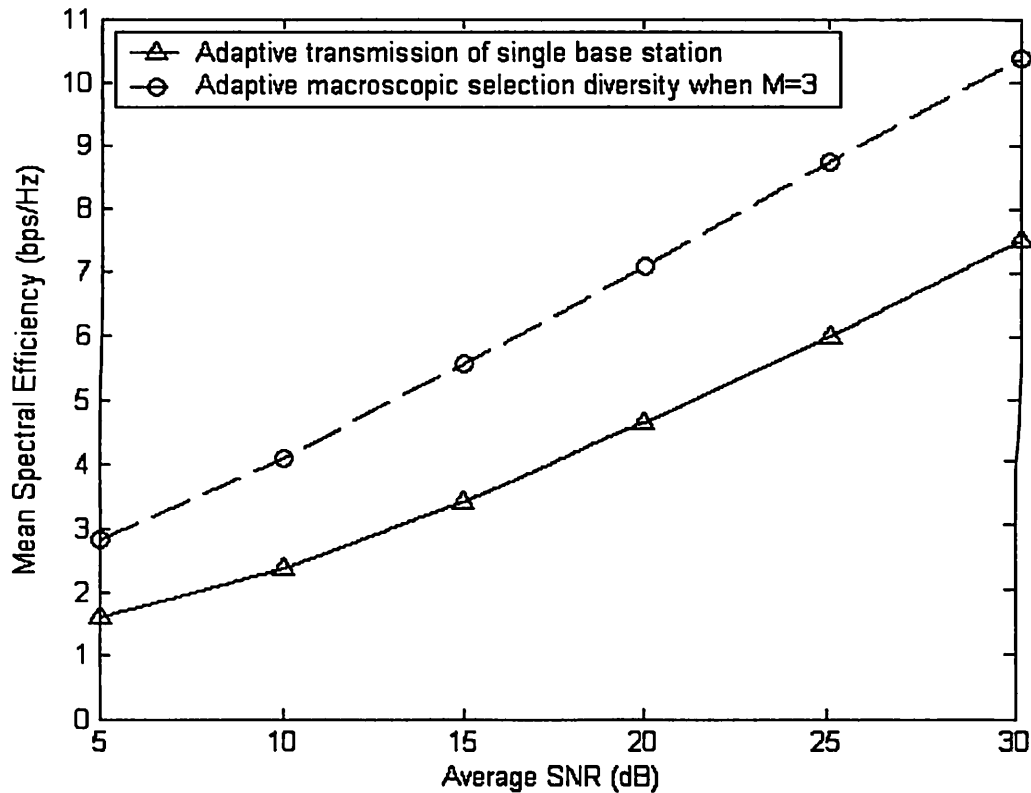
Fig. 4.6 Mean spectral efficiency comparison between the macroscopic selection diversity and a single base station for C-Rate I-BER case at target BER of 10^{-3}.

In the above figure, M is the number of branches for the selection diversity. It has been shown that the spectral efficiency increases significantly when we deploy more base stations to support one cell. At the same time, if we fix the spectral efficiency to 5 bps/Hz, involving more base stations, the minimum SNR required to support the average BER as 10^{-3} is much smaller than the case of a single base station topology. This means that by applying the macroscopic selection diversity, we support BER constraint-based wireless services at a certain SNR level that is much less than the required SNR for a single base

station [35]. Such a system can provide robust and reliable wireless data link even under low SNR. For example, in Fig. 4.6, to support 5 bps/Hz data rate, the single base station system needs the average SNR at around 22 dB; but the required SNR of a macroscopic selection diversity system needs only 13 dB.

4.2.2 Adaptive Macroscopic MRC Scheme

As we know, the selection diversity is the simplest diversity scheme, but it also provides the worst capacity performance as we discard other base station resources. It has been shown in Chapter 2, that the MRC diversity scheme gives the best performance among those three receiver diversity schemes. Therefore, the spectral efficiency performance of the adaptive macroscopic MRC scheme is analyzed in this section.

Similar to last section, the PDF of joint instantaneous SNR γ of several base stations needs to be taken into the Lagrange equations for different constraints. Unfortunately, the close form PDF representation of joint composite Rayleigh plus log-normal distributed SNR is not known. In order to solve this problem, the Monte Carlo simulation is used to evaluate a suboptimal adaptation for C-Rate I-BER case. In the optimal case, if the channel is distorted seriously, the system would allocate less power or zero power if the SNR is below the cutoff fade. The power thus saved will be distributed to the channel when it is in good condition. In the suboptimal case, the total power for each transmission is fixed. In each transmission, the total power is equally allocated to all available base stations. Since the transmit power is fixed, the equation (4.13) can be changed to

$$k(\gamma) = \begin{cases} \dfrac{1}{c_3}\log_2\left[c_4 - \dfrac{c_2\gamma}{\ln(\frac{\overline{BER}}{c_1})}\right], & k(\gamma) \geq 0 \\ \qquad\qquad 0 & else \end{cases} \qquad (4.30)$$

In the suboptimal case, for the selection diversity scheme, the instantaneous SNR γ in (4.30) is the largest instantaneous SNR from all base stations; for the MRC scheme, the γ in (4.30) is the summation of instantaneous SNR of all base stations. To calculate the mean spectral efficiency of the suboptimal case for C-Rate I-BER constraint, the statistics of the instantaneous SNR under composite fading is generated. Using (4.30), the statistics and mean value of instantaneous spectral efficiency can be obtained.

The mean spectral efficiencies of the suboptimal case for a composite fading channel versus the average SNR for two different constraints with the macroscopic three-branch MRC diversity combining and the three-branch selection diversity when instantaneous BER is 10^{-3} are shown in Fig. 4.8. Before that, the comparison between the optimal case and the suboptimal case for the macroscopic selection diversity scheme under composite fading with C-Rate I-BER constraint is demonstrated in Fig. 4.7.
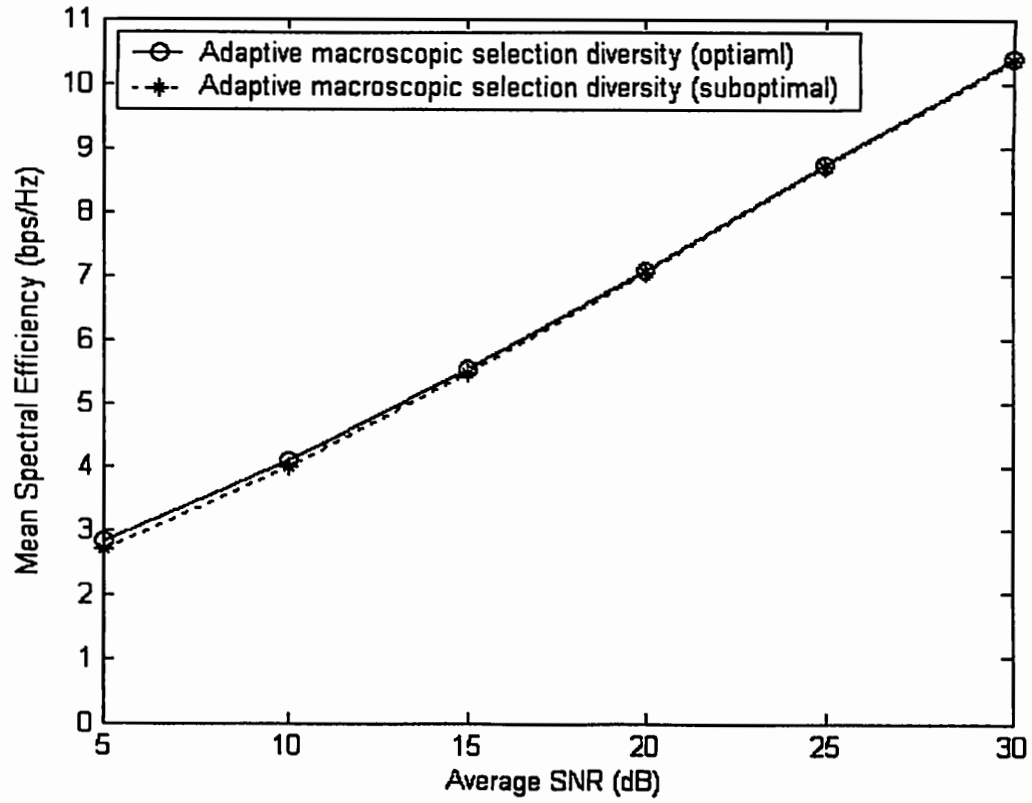
Fig. 4.7 Comparison between the optimal case and the suboptimal case for the macroscopic selection diversity scheme under the composite fading with C-Rate I-BER constraint.
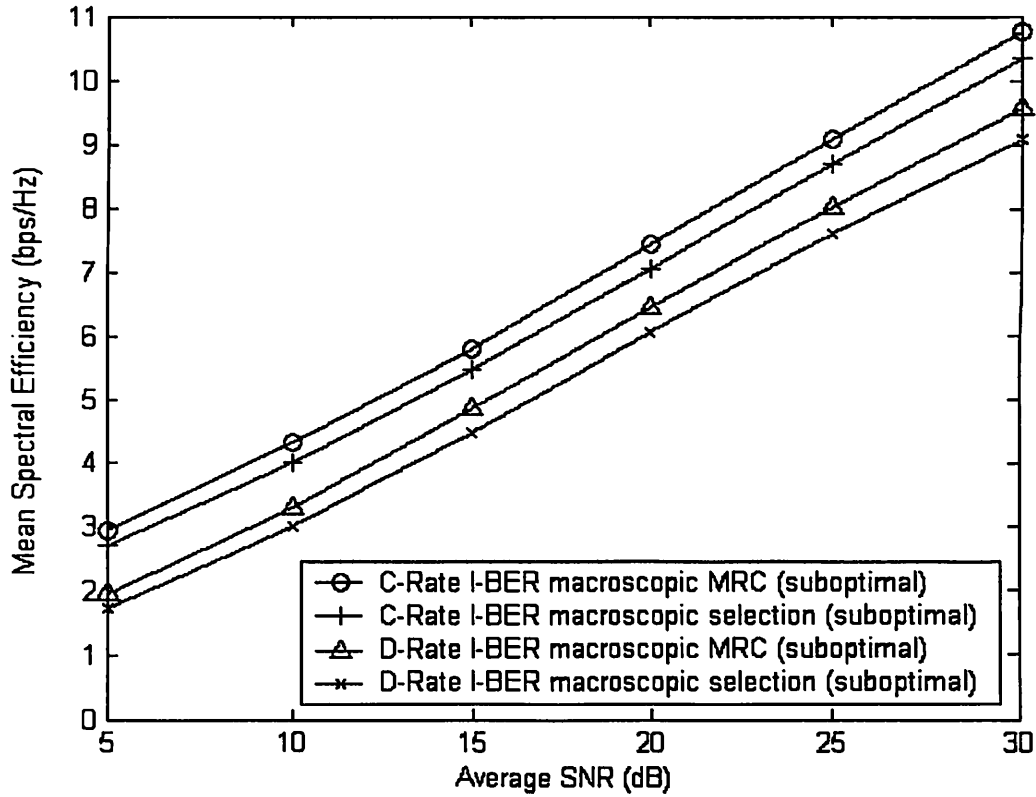
Fig. 4.8 Mean spectral efficiency of the suboptimal scheme for a composite fading channel versus the average SNR for two different constraints with the macroscopic three-branch MRC diversity combining and the selection diversity when the instantaneous BER is 10^{-3}.

As shown in Fig. 4.7, the curve of the suboptimal case for the adaptive macroscopic selection diversity scheme derived from Monte Carlo simulation is very close to the curve of the optimal case, which means that there is not much penalty between our assumption and ideal adaptive scheme. This conforms to the discussion in [5], which states that using just one or two degrees of freedom in adaptive modulation yields close to the maximum possible spectral efficiency obtained by utilizing all degrees

of freedom.

Fig. 4.8 shows that the macroscopic MRC scheme has better spectral efficiency performance compared to that of the selection diversity scheme for both constraints at any average SNR. Another observation is that the performance of diversity schemes under C-Rate I-BER case has about 1 bps/Hz larger than that of diversity schemes under D-Rate I-BER. Since in the real adaptive transmission system the signal constellation size can only be an integer, the D-Rate I-BER constraint is more practical.

Chapter 5

Conclusions

This thesis proposes two kinds of optimized wireless mobile communication systems: the macroscopic MIMO system and the adaptive macroscopic diversity system.

In Chapter 3, it is shown that the MIMO system capacity increases linearly compared to the SISO system when the channel characteristics are i.i.d. fading. When the fading channels are correlated, the capacity of the MIMO system will be reduced dramatically. The channel correlation can result from the small angle spread, close surrounding scatterers, or the lack of antenna spacing. In the correlated fading case, the MIMO system can be decomposed into $\min(M, N)$ number of single channel subsystems, where M and N are the number of antennas at the transmitter and receiver, respectively. If the CSI is known at the transmitter, the water-filling power allocation strategy can be applied to optimize the system capacity. In the MIMO-MDC system, some independent fading channels can be obtained due to the sparsely distributed base stations. The simulation results show that the capacity of the MIMO-MDC system is increased significantly compared to the single base station MIMO system. The results also indicate that the deployment of the transmit antennas at several geographically distributed base stations can provide more capacity than deploying all the antennas at one base station. This is because the MIMO-MDC system can maximize the spatial multiplexing gain

67

while combating the Rayleigh fading by deploying multiple antennas at the receiver and mitigating the log-normal shadowing effect by combining independent signals from different base stations.

Chapter 4 applies the adaptive transmission technology to the macroscopic diversity system to optimize the spectral efficiency under the BER constraint. By taking the PDF of the macroscopic selected SNR of the composite fading channel to the Lagrange equations for different constraints, the spectral efficiencies can be obtained. It has been shown that the spectral efficiency increases significantly when we deploy more base stations to support one cell for all constraints. Meanwhile, by applying the macroscopic selection diversity, the topology can support BER constraint-based wireless services at SNR levels that are much less than the required SNR levels when using a single base station. Thus we can conclude that the macroscopic topology improves the QoS of wireless network especially when the channel condition significantly varies (i.e., the SNR may fluctuate). In the following section, applications of the adaptive transmission with the macroscopic MRC system is presented, where a suboptimal case is proposed because the joint PDF of the composite Rayleigh plus log-normal distributed SNR is not known. Although the transmit power is fixed for each transmission, the performance of the suboptimal case is very close to that of the optimal case. This means that there is no significant penalty when using the suboptimal scheme instead of the optimal one. The following section investigated the mean spectral efficiencies of the suboptimal optimization scheme for a composite fading channel versus the average SNR for two the different constraints, with the macroscopic three-branch MRC diversity combining and the selection diversity, for an instantaneous BER requirement of 10^{-3}. The macroscopic

MRC scheme has a better spectral efficiency performance compared to that of the selection diversity scheme for both the C-Rate I-BER and the D-Rate I-BER constraints at any average SNR level. As a conclusion, the adaptive macroscopic MRC scheme seems to be the best choice to provide high spectral efficiency. Although, this performance gain is obtained with a higher complexity cost of the combining system compared to a selection diversity based topology.

Chapter 6

References

[1] J. Winters, "On the capacity of radio communication systems with diversity in a Rayleigh fading environment," *IEEE J. Select. Areas Commun.*, vol. 5, pp. 871-878, June 1987.

[2] G. J. Foschini, "Layered space-time architecture for wireless communication in fading environments when using multi-element antennas," *Bell Labs Tech. J.*, pp. 41-59, 1996.

[3] E. Telatar, "Capacity of multi-antenna Gaussian channels," *Eur. Trans. Telecomm. ETT*, vol. 10, no. 6, pp. 585-596, Nov.1999.

[4] A. J. Goldsmith and S.-G. Chua, "Variable-rate variable-power MQAM for fading channels," *IEEE Trans. Commun.*, vol. 45, pp. 1218-1230, Oct. 1997.

[5] S. T. Chung and A. J. Goldsmith, "Degrees of freedom in adaptive modulation: A unified view," *IEEE Trans. Commun.*, vol. 49, no. 9, pp. 1561-1571, Sept. 2001.

[6] J. G. Proakis, *Digital Communications*, 4th ed. New York: McGraw-Hill, 2000.

[7] A. Abu-Dayya, N. C. Beaulieu, "Outage Probabilities in the Presence of Correlated Lognormal Interferers," *IEEE Trans. Veh. Technol.*, vol. 43, no. 1, pp. 164- 173, Feb. 1994.

[8] G. L. Stuber, *Principles of Mobile Communication*, 2nd ed. Norwell, MA: Kluwer, 2001.

[9] W. C. Y. Lee and Y. S. Yeh, "On the estimation of the second-order statistics of log-normal fading in mobile radio environment," *IEEE Trans. Commun.*, vol. 22, pp.809-873, June 1974.

[10] http://www.its.bldrdoc.gov/fs-1037/dir-026/_3783.htm

[11] M. G. Linnartz, "Exact Analysis of the Outage Probability in Multiple-User Mobile Radio," *IEEE Trans. Commun.*, vol. 40, no. 1, pp. 20-23, Jan. 1992.

[12] G. Karagiannidis, S. Kotsopoulos, and C. Georgopoulos, "Outage Probability Analysis for a Rician Signal in L Nakagami Interferers with Arbitrary Parameters," *IEEE J. Commun. and Netw.*, vol. 1, no. 1, pp. 26-30, Mar. 1999.

[13] A. Ganesan and A. M. Sayeed, "A Virtual Input-Output Framework for Tranceiver Analysis and Design for Multipath Fading Channels," *IEEE Trans. Commun.*, vol. 51, no. 7, pp. 1149-1160, July 2003.

[14] G. J. Foschini and M. J. Gans, "On limit of wireless communications in fading environment when using multiple antennas," *Wireless Personal Commun.*, vol. 6, no. 3, pp. 311–335, June 1998.

[15] Y.Z. Xie and C. N. Georghiades, "Minimum Outage Probability Transmission with Imperfect Feedback for MISO Fading Channels," http://ee.tamu.edu/~yzxie/min_out_v6.pdf.

[16] E. Biglieri, J. Proakis and S. S. (Shitz), "Fading Channels: Information-Theoretic and Communications Aspects," *IEEE Trans. Inform. Theory*, vol. 44, no. 6, pp. 2619-2692, Oct. 1998.

[17] H. Bölcskei, D. Gesbert and A. J. Paulraj, "On the Capacity of OFDM-Based Spatial Multiplexing Systems," *IEEE Trans. Commun.*, vol. 50, no. 2, pp. 225-234, Feb. 2002.

[18] M. T. Ivrlajc, W. Utschick and J.A. Nossek, "Fading Correlations in Wireless MIMO Communication Systems," *IEEE J. Select Areas Commun.*, vol. 21, no. 5, pp. 819-828, June 2003.

[19] K. K. Mukkavilli, etc., "On the Outage Probability of a Class of Signaling Schemes for Multiple Antennas," *IEEE Inter. Symp. Inform. Theory*, July 2002.

[20] A. Goldsmith, S. Jafar, N. Jindal, and S. Vishwanath, "Capacity limits of MIMO channels," *IEEE J. Select. Areas Commun.*, vol. 21, no. 5, pp. 684-702, June 2003.

[21] A. Lozano, F. Farrokhi, and R. Valenzuela, "Lifting the limits on high-speed wireless data access using antenna arrays," *IEEE Commun. Magzine*, pp. 156-162, September 2001.

[22] D. Shiu, *Wireless Communication using Dual Antenna Arrays*. MA: Kluwer, 2000.

[23] D. Gesbert, H. Blocskei, D. Gore, and A. Paulraj, "Outdoor MIMO wireless channels: models and performance prediction," *IEEE Trans. Commun.*, vol. 50, issue: 12, pp. 1926-1934, December 2002.

[24] D. Chizhik, J. Ling, P. Wolniansky, R. Valenzuela, N. Costa, and K. Huber, "Multiple input multiple output measurements and modeling in Manhattan," in *Proc. IEEE Vehicular Technology Conf.*, 2002, pp. 107-110.

[25] V. Tarokh, N. Seshadri, and A. R. Calderbank, "Space–time codes for high data rate wireless communication: Performance analysis and code construction," *IEEE Trans. Inform. Theory*, vol. 44, no. 2, pp. 744–765, Mar. 1998.

[26] W. C. Jakes, Jr., *Microwave Mobile Communications*. New York, NY: John, 1974.

[27] Z. J. Hass and C.-P. Li, "The multiply-detected macrodiversity scheme for wireless cellular systems," *IEEE Trans. Veh. Technol.*, vol. 47, no. 2, pp. 506-530, May 1998.

[28] A. M. D. Turkmani, "Performance evaluation of a composite microscopic plus macroscopic diversity system," *Proc. Inst. Elect. Eng.-I Commun., Speech and Visions,* vol. 138, no. 1, pp. 15-20, Feb. 1991.

[29] A. M. D. Turkmani, " Probability of error for M-branch macroscopic selection diversity," *Proc. Inst. Elect. Eng.-I Commun., Speech and Visions,* vol. 139, no. 1, pp. 71-78, Feb. 1992.

[30] M.-S. Alouini, A. J. Goldsmith, "Capacity of Rayleigh fading channels under different adaptive transmission and diversity-combining techniques," *IEEE Trans. Veh. Technol.,* vol. 48, no. 4, pp. 1165-1181, July 1999.

[31] N. Krishnan, *Matrix algebra: an introduction,* Beverly Hills: Sage, 1984.

[32] J. Chung, C.-S. Hwang, K. Kim, and Y. K. Kim. "A random beamforming technique in MIMO systems exploiting multiuser diversity," *IEEE J. Select. Areas Commun.,* vol. 21, no. 5, pp. 848-855, June 2003.

[33] R. Ertel, P. Cardieri, K. Sowerby, T. Rappaport, and J. Reed, "Overview of spatial channel models for antenna array communication systems," *IEEE Personal Commun.,* pp. 10-22, Feb. 1998.

[34] W. H. Press, etc., *Numerical Recipes in C: The Art of Scientific Computing,* 2nd ed. Cambridge, UK, 1992.

[35] J.-M. Chung, W.-C. Jeong, K. Ramasamy and R. Ramasamy, "Enhanced robust wireless network QoS control applying adaptive modulation and macroscopic diversity combining techniques," in *Proc. IEEE Consumer Communications and Networking Conf.,* 2004, pp. 228-232.

Appendix A

Derivations of Adaptive Modulation Optimization Equations for

Different Constraints

The proof of the equations given in section 4.1.1 for three different constraints, C-Rate A-BER, C-Rate I-BER, and D-Rate I-BER, is provided below.

A1. Derivation for C-Rate A-BER case

The Lagrange equation for C-Rate A-BER case that is constrained by the average power constraint and average BER constraint is

$$
\begin{aligned}
J(k(\gamma), S(\gamma)) = &\int_0^\infty k(\gamma)p(\gamma)d\gamma + \lambda_1 [\int_0^\infty BER(\gamma)k(\gamma)p(\gamma)d\gamma - \overline{BER}\int_0^\infty k(\gamma)p(\gamma)d\gamma] \\
&+ \lambda_2 [\int_0^\infty S(\gamma)p(\gamma)d\gamma - \overline{S}]
\end{aligned}
\tag{A.1}
$$

The optimal rate and power adaptation should satisfy

$$
\frac{\partial J}{\partial k(\gamma)} = 0 \text{ and } \frac{\partial J}{\partial S(\gamma)} = 0
\tag{A.2}
$$

where

$$
BER(\gamma) \approx c_1 \exp\left[\frac{-c_2\gamma\frac{S(\gamma)}{\overline{S}}}{f(k(\gamma))}\right] \text{ and } f(k(\gamma)) = 2^{c_3 k(\gamma)} - c_4
\tag{A.3}
$$

$$\frac{\partial J}{\partial k(\gamma)} = 1 + \lambda_1 \left[BER(\gamma) + k(\gamma) \frac{\partial(BER(\gamma))}{\partial k(\gamma)} - \overline{BER} \right]$$

$$= 1 + \lambda_1 \left\{ BER(\gamma) + k(\gamma) \frac{c_1 c_2 \gamma S(\gamma)/\overline{S}}{[f(k(\gamma))]^2} \frac{\partial f(k(\gamma))}{\partial k(\gamma)} \exp\left[\frac{-c_2 \gamma S(\gamma)/\overline{S}}{f(k(\gamma))} \right] - \overline{BER} \right\} \quad (A.4)$$

$$= 1 + \lambda_1 \left(BER(\gamma) \left[1 + \frac{k(\gamma) c_2 \gamma S(\gamma)/\overline{S}}{[f(k(\gamma))]^2} \frac{\partial f(k(\gamma))}{\partial k(\gamma)} \right] - \overline{BER} \right) = 0$$

$$\frac{\partial J}{\partial S(\gamma)} = \lambda_1 \frac{\partial BER(\gamma)}{\partial S(\gamma)} k(\gamma) + \lambda_2 = -\frac{\lambda_1 c_2 \gamma k(\gamma)}{\overline{S} f(k(\gamma))} BER(\gamma) + \lambda_2 = 0 \quad (A.5)$$

From (A.5), the optimized BER equation can be obtained

$$BER(\gamma) = \frac{\lambda_2 \overline{S} f(k(\gamma))}{\lambda_1 c_2 \gamma k(\gamma)} \quad (A.6)$$

Substituting (A.6) into (A.4), the power adaptation that maximizes the spectral efficiency should satisfy

$$\frac{S(\gamma)}{\overline{S}} = \max\left[\frac{f(k(\gamma))}{\frac{\partial f(k(\gamma))}{\partial k(\gamma)} \lambda_2 \overline{S}} (\lambda_1 \overline{BER} - 1) - \frac{f(k(\gamma))^2}{c_2 \gamma \frac{\partial f(k(\gamma))}{\partial k(\gamma)} k(\gamma)}, 0 \right] \quad (A.7)$$

where $\dfrac{S(\gamma)}{\overline{S}}$ is the ratio between the instantaneous transmit power and the average power.

From (A.3), (A.6), and (A.7), the rate adaptation $k(\gamma)$ can be obtained as either zero or the nonnegative solution of

$$\frac{\lambda_1 \overline{BER} - 1}{\frac{\partial f(k(\gamma))}{\partial k(\gamma)} \lambda_2 \overline{S}} - \frac{f(k(\gamma))}{c_2 \gamma \frac{\partial f(k(\gamma))}{\partial k(\gamma)} k(\gamma)} = \frac{1}{\gamma c_2} \ln\left[\frac{\lambda_1 c_1 c_2 \gamma k(\gamma)}{\lambda_2 \overline{S} f(k(\gamma))} \right] \quad (A.8)$$

A2. Derivations for C-Rate I-BER case

The instantaneous BER constraint is $BER(\gamma) = \overline{BER}$, so by inverting (A.3), $k(\gamma)$

can be expressed as a function of the adaptive power $S(\gamma)$ and the fixed bit error rate

$$k(\gamma) = \begin{cases} \dfrac{1}{c_3} \log_2 \left[c_4 - \dfrac{c_2 \gamma}{\ln(\frac{\overline{BER}}{c_1})} \dfrac{S(\gamma)}{\overline{S}} \right], & S(\gamma) \ge 0, k(\gamma) \ge 0 \\ 0 & else \end{cases} \tag{A.9}$$

To maximize spectral efficiency, the Lagrange equation becomes

$$J(S(\gamma)) = \int_0^\infty k(\gamma) p(\gamma) d\gamma + \lambda [\int_0^\infty S(\gamma) p(\gamma) d\gamma - \overline{S}] \tag{A.10}$$

The optimal power should satisfy

$$\frac{\partial J}{\partial S(\gamma)} = 0, \quad S(\gamma) \ge 0, \quad k(\gamma) \ge 0 \tag{A.11}$$

By solving $\dfrac{\partial J}{\partial S(\gamma)} = \dfrac{\partial k(\gamma)}{\partial S(\gamma)} + \lambda = 0$, the optimal power adaptation is

$$\frac{S(\gamma)}{\overline{S}} = \begin{cases} -\dfrac{1}{c_2 (\ln 2) \lambda \overline{S}} - \dfrac{1}{\gamma K}, & S(\gamma) \ge 0 \\ 0 & else \end{cases} \tag{A.12}$$

where K is given as

$$K = -\frac{c_2}{c_4 \ln\left(\dfrac{\overline{BER}}{c_1}\right)} \tag{A.13}$$

(A. 12) can be simplified as

$$\frac{S(\gamma)}{\overline{S}} = \begin{cases} \dfrac{1}{\gamma_0 K} - \dfrac{1}{\gamma K}, & S(\gamma) \ge 0 \\ 0 & else \end{cases} \tag{A.14}$$

where $\gamma_0 \ge 0$ is the cutoff fade depth that can be obtained by substituting (A.14) into

average power constraint and solving the following equation

$$\int_{\gamma_0}^{\infty} \frac{1}{K} \left[\frac{1}{\gamma_0} - \frac{1}{\gamma} \right] p(\gamma) dr = 1 \qquad (A.15)$$

A3. Derivations for D-Rate I-BER case

In reference to [5], the transmission rate is assumed to be selected from the set $\{k_i\}_{i=0}^{N-1} = \{0\ 2\ 4\ 6\ 8\ 10\ 12\}$, which means $N=7$. The same rate k_i is assigned when the instantaneous SNR is in the region $[\gamma_i, \gamma_{i+1})$. Since $BER(\gamma) = \overline{BER}$, by modifying (A.3), the power adaptation can be written as

$$\frac{S(\gamma)}{\overline{S}} = \frac{h(k_i)}{\gamma} \qquad (A.16)$$

where $h(k_i) = -\frac{1}{c_2} \ln\left(\frac{\overline{BER}}{c_1} \right) f(k_i)$.

The Lagrange method is still applied to find the optimal region boundaries that maximize spectral efficiency. The equation is

$$J(\gamma_i) = \sum_{0 \le i \le N-1} k_i \int_{\gamma_i}^{\gamma_{i+1}} p(\gamma) d\gamma + \lambda \left[\sum_{0 \le i \le N-1} \int_{\gamma_i}^{\gamma_{i+1}} \frac{h(k_i)}{\gamma} p(\gamma) d\gamma - 1 \right] \qquad (A.17)$$

Then differentiating (A.17), it becomes

$$\frac{\partial J}{\partial \gamma_i} = k_{i-1} - k_i + \lambda \left[\frac{h(k_{i-1})}{\gamma_i} - \frac{h(k_i)}{\gamma_i} \right] = 0 \qquad (A.18)$$

So the optimal rate region boundaries can be obtained from (A.18) as

$$\gamma_i = \begin{cases} \dfrac{h(k_0)}{k_0} \rho, & i = 0 \\[2mm] \dfrac{h(k_i) - h(k_{i-1})}{k_i - k_{i-1}} \rho, & 1 \le i \le N-1 \end{cases} \qquad (A.19)$$

In (A.19), $\rho = -\lambda$ is determined by the average power constraint.

76

VITA ①

Yuan Zhang

Candidate for the Degree of

Master of Science

Thesis: PERFORMANCE ANALYSIS OF ADAPTIVE MODULATION AND MIMO SYSTEMS APPLYING MACROSCOPIC DIVERSITY TECHNOLOGIES

Major Field: Electrical Engineering

Biographical:

Personal Data: Born in Wu Han, China, On February 4, 1979.

Education: Received Bachelor of Engineering degree in Electrical Engineering from Wuhan University of Technology, China, in June 2001. Completed the requirements for the Master of Science degree with a major in Electrical and Computer Engineering at the Oklahoma State University in July 2004.

Experience: Graduate Research Assistant in the school of Electrical and Computer Engineering, Oklahoma State University, Stillwater, Oklahoma, January 2003 to July 2004.

Graduate Teaching Assistant in the school of Electrical and Computer Engineering, Oklahoma State University, Stillwater, Oklahoma, August 2003 to July 2004.

Technical Support Engineer in HUAWEI TECHNOLOGIES CO. LTD., China, July 2001 to June 2002.